
Article:
Oochi, A, Hajny, J, Fukui, K et al. (2019) Pinstatic Acid Promotes Auxin Transport by Inhibiting PIN Internalization. Plant Physiology, 180 (2). pp. 1152-1165. ISSN: 0032-0889

https://doi.org/10.1104/pp.19.00201

Short title

Pinstatic acid is a modulator of PIN trafficking.

Corresponding author details

Ken-ichiro Hayashi, Ph.D.

Professor, Department of Biochemistry, Okayama University of Science, 1-1 Ridai-cho, Okayama 700-0005, Japan

Title

Pinstatic acid promotes auxin transport by inhibiting PIN internalization

Authors

Akihiro Oochi,[a] Jakub Hajny,[b,h] Kosuke Fukui,[a] Yukio Nakao,[a] Michelle Gallei, [b] Mussa Quareshy,[c] Koji Takahashi,[de] Toshinori Kinoshita,[de] Sigurd Ramans Harborough,[f] Stefan Kepinski,[f] Hiroyuki Kasahara,[g] Richard Napier,[c] Jiri Friml,[b] Ken-ichiro Hayashi[a1]

[a]Department of Biochemistry, Okayama University of Science, Okayama 700-0005, Japan.

[b]Institute of Science and Technology Austria, Klosterneuburg, Austria.

[c]School of Life Sciences, University of Warwick, Coventry, CV4 7AL, United Kingdom

[d]Graduate School of Science, Nagoya University, Chikusa, Nagoya, 464-8602 Japan.

[e]Institute of Transformative Bio-Molecules (WPI-ITbM), Nagoya University, Chikusa, Nagoya, 464-8601, Japan.

[f]Centre for Plant Sciences, Faculty of Biological Sciences, University of Leeds, Leeds LS2 9JT, UK.

[g]Institute of Global Innovation Research, Tokyo University of Agriculture and Technology, Fuchu-shi, Tokyo 183-8509, Japan

[h]Laboratory of Growth Regulators, The Czech Academy of Sciences, Institute of Experimental Botany & Palacký University, Šlechtitelů 27, CZ-78371 Olomouc, Czech Republic

One sentence summary

Pinstatic acid is an inactive auxin analog for the SCF(TIR1/AFB) pathway that positively modulates auxin efflux transport by inhibiting PIN internalization.

Author contribution

A.O. J.H., J.F., Y.N., and K.H. conceived this project and designed research, discussed the data, R.N., S.K., J.F., and K.H. wrote the paper; rapid hypocotyl elongation assay were performed by T.K., K.T., ; Endogenous IAA analysis was performed by H.K.; surface plasmon resonance assays were

performed by M.Q. and R.N.; pull-down assays were performed by S.R.H. and S.K.; all other experiments were performed by A.O., J.H., M.G., F.K., J.F., Y.N., and K.H..

Funding information

This work was supported in part by the Ministry of Education, Culture, Sports, Science, and Technology through a Grant-in-Aid for Scientific Research (no. JP25114518 to K.H.), BBSRC award BB/L009366/1 to R.N. and S.K. and European Union's Horizon2020 program (ERC grant agreement n° 742985) to J.F.

Corresponding author email

hayashi@dbc.ous.ac.jp

Keywords

Auxin, PIN, polar transport, small molecule, Arabidopsis thaliana, receptor, membrane transport

ABSTRACT

Polar auxin transport plays a pivotal role in plant growth and development. PIN auxin efflux carriers are major mediators for directional auxin movement establishing local auxin maxima, minima, and gradients that drive multiple developmental processes and responses to environmental signals. Auxin has been proposed to modulate its own transport by regulating subcellular PIN trafficking including clathrin-mediated PIN endocytosis and constitutive recycling. The mechanism of auxin's effect on PIN trafficking remains elusive. To dissect the regulatory mechanism of PIN trafficking by auxin, we screened auxin analogs and identified pinstatic acid (PISA) as a positive modulator of polar auxin transport. PISA shows auxin-like activity for hypocotyl elongation and adventitious root formation via positive regulation of auxin transport. PISA is inert for $SCF^{TIR1/AFB}$ signaling and yet induces PIN accumulation at the cell surface by inhibiting PIN internalization from the plasma membrane. PISA is thus a new promising chemical tool to dissect the regulatory mechanism of subcellular PIN trafficking and auxin transport.

INTRODUCTION

The plant hormone auxin is a master regulator of plant growth and development. Indole 3-acetic acid (IAA), the predominant natural auxin regulates numerous and diverse developmental processes such as establishment of embryo polarity, vascular differentiation, apical dominance and tropic responses to light and gravity (Hayashi, 2012). The auxin responses regulating these diverse developmental events can be modulated at three major steps: auxin metabolism (Korasick et al., 2013; Kasahara, 2016), directional auxin transport (Adamowski and Friml, 2015) and signal transduction (Leyser, 2018).

Polar auxin transport plays a crucial role in auxin-regulated development by influencing local auxin maxima and gradients and is mediated principally by three families of membrane proteins, the Auxin1/Like Aux1 (AUX1/LAX) auxin influx carriers, the PIN-FORMED (PIN) auxin efflux facilitators and several members of the ATP-binding cassette group B (ABCB) auxin transporters (Adamowski

and Friml, 2015).

The polar subcellular localization of the auxin efflux machinery determines the directionality of auxin flow. The spatiotemporal regulation of auxin gradients also depends on the cell-specific expression and subcellular localization of plasma membrane (PM)-localized PIN proteins (PIN1 - PIN4 and PIN7), the latter often being responsive to environmental and developmental cues (Adamowski and Friml, 2015). PIN proteins are often asymmetrically distributed within the cell and are constantly recycled between endosomal compartments and PM. The dynamics of polar localization of PIN proteins regulates the rate and direction of cellular auxin export and this ultimately determines auxin gradients in the tissue. Therefore, the regulatory machinery of the polarity and abundance of PM-localized PIN proteins are crucial for diverse developmental processes and morphogenesis including embryogenesis, initiation of lateral organs, and tropic responses (Robert et al., 2013; Adamowski and Friml, 2015; Rakusova et al., 2015).

The exocytosis and endocytosis of PIN proteins at the PM can be modulated by ADP RIBOSYLATION FACTOR-GUANINE NUCLEOTIDE EXCHANGE FACTORS (ARF-GEFs) including GNOM (Naramoto et al., 2010). PIN proteins are internalized from the PM to the trans-Golgi network / early endosome (TGN/EE) compartments and then PINs can proceed along the recycling route to the PM (Adamowski and Friml, 2015). An important tool for investigating exocytic protein sorting is Brefeldin A (BFA), which is a reversible inhibitor of ARF-GEFs including GNOM (Geldner et al., 2001; Geldner et al., 2003). BFA treatment leads to accumulation of the endocytosed PINs in artificial intracellular aggregates called BFA bodies, the formation of which can be reversed by washing out the BFA (Geldner et al., 2001).

Clathrin-mediated endocytosis is also involved in the internalization of PIN proteins from the PM (Kitakura et al., 2011; Adamowski et al., 2018) and is modulated by the ROP (Rho guanidine triphosphate hydrolases of plants) family of Rho-like GTPases and their associated RICs (ROP interactive CRIB motif-containing proteins) (Lin et al., 2012; Nagawa et al., 2012). Genetic analysis has revealed that MAB4 (MACCHI-BOU4)/ ENP (ENHANCER OF PID)/NPY1(NAKED PINS IN

YUCCA-like1), a gene encoding NPH3 (NON-PHOTOTROPIC HYPOCOTYL3)-like proteins and homologous MELs (MAB4/ENP/NPY1-like), regulates PIN abundance at the PM (Furutani et al., 2014). The internalization and trafficking of PIN proteins is dynamically regulated by developmental and environmental cues, such as plant hormones, gravity and light (Ding et al., 2011; Rakusova et al., 2016). Short-term auxin treatments, in particular using synthetic auxin analogs, blocks clathrin-mediated internalization of PIN proteins from the PM and consequently enhances PIN abundance at the PM and increases auxin efflux (Paciorek et al., 2005; Robert et al., 2010). Auxin also induces PIN1 relocalization from basal to the inner lateral PM of root endodermal and pericycle cells (Prat et al., 2018). Similarly, auxin mediates PIN3 relocalization during gravitropic response to terminate gravitropic bending (Rakusova et al., 2016). Prolonged auxin treatment induces PIN2 vacuolar targeting and degradation, and this is mediated by the $SCF^{TIR1/AFB}$ pathway (Abas et al., 2006; Baster et al., 2013), which presumably also explains the $SCF^{TIR1/AFBs}$-dependent auxin effect on PIN2-GFP accumulation in BFA bodies (Pan et al., 2009). In addition, auxin has been reported to reduce the abundance of photoconvertible PIN2-Dendra at the PM by repressing the translocation of newly synthesized PIN2 to the PM (Jasik et al., 2016). Besides auxin effect on PIN trafficking, also other hormones including Cytokinin (Marhavy et al., 2011), Salicylic acid (Du et al., 2013), Gibberellic acid (Salanenka et al., 2018) can influence different aspect of PIN trafficking providing a possible entry points for crosstalk of these signaling pathways with auxin distribution network.

Given these different and sometimes contradictory observations for different PINs in different cells and using different approaches, the underlying cellular and molecular mechanisms for the targeting and recycling of PIN proteins, and in particular for their regulation by auxin, remain largely unknown.

To develop a useful chemical tool for dissecting the regulatory mechanism of PIN trafficking, we have screened phenylacetic acid (PAA) derivatives for selective modulation of PIN trafficking. We identified 4-ethoxyphenylacetic acid which was designated as PInStatic Acid (PISA) due to its activity on PIN-mediated polar auxin transport. PISA shows auxin-like activity for hypocotyl elongation and

adventitious root formation by positively modulating auxin transport. Similar to conventional auxins, PISA blocks the internalization of PIN proteins from the PM and consequently induces PIN protein accumulation at the PM. PISA is notably different from other known auxin chemical tools, like auxin transport inhibitors 2,3,5 - triiodobenzoic acid (TIBA) and N-1-naphthylphthalamic acid (NPA). Therefore, PISA represents a promising chemical tool for dissecting the complicated regulations of PIN trafficking by auxin.

RESULTS

Pinstatic acid is an inactive PAA analog on TIR1/AFB-Aux/IAA co-receptor complex.

Auxins modulate the expression and degradation of PIN proteins via the $SCF^{TIR1/AFB}$ signaling pathway (Baster et al., 2013; Ren and Gray, 2015). On the other hand, clathrin-mediated endocytosis of PIN is inhibited by auxin via a non-transcriptional pathway (Robert et al., 2010). These positive and negative effects of auxin on PIN trafficking hinder access to the regulatory components in PIN trafficking using conventional genetic approaches. Therefore, we searched for an auxin transport modulator that would make PIN trafficking more amenable to experimentation. To this end, we initially screened PAA derivatives according to following criteria; (i) The derivative should be inactive on the $SCF^{TIR1/AFB}$ pathway and (ii) derivative treatment should induce auxin-related phenotypes that are different from the phenotypes typical of auxins or auxin transport inhibitors, such as TIBA and NPA.

In the course of screening, we found that 4-ethoxyphenylacetic acid (later denoted PISA) promoted hypocotyl elongation but did not induce auxin-responsive *DR5::GUS* reporter gene expression which is mediated by the $SCF^{TIR1/AFB}$ pathway (Fig. 1A, 1C and 2). Thus, PISA was selected as the most promising candidate from a series of 4-alkyloxy-PAA derivatives and further characterized in detail.

Auxin is biosynthesized by two enzymes, TAA1 and YUC in the indole 3-pyruvic acid (IPA) pathway (Kasahara, 2016). The inhibition of this pathway by L-kynurenine (Kyn), a TAA1 inhibitor,

158 and yucasin DF, a YUC inhibitor, caused short and curled roots that are typical auxin-deficient
159 phenotypes (Fig. 1B) (He et al., 2011; Tsugafune et al., 2017). A quintuple *yuc 3 5 7 8 9* mutant
160 showed a similar auxin-deficient root phenotype (Fig. S1A) (Chen et al., 2014). IAA and
161 1-naphthylyacetic acid (NAA) at 50-100 nM recovered these auxin-deficient root defects in root
162 elongation and gravitropism (Fig. 1B and S1A). 3-Ethoxyphenylacetic acid (meta-substituted PISA:
163 mPISA), an analog of PISA (Fig. 1A) that retains weak auxin activity in *DR5::GUS* expression (Fig.
164 1C) also rescued the auxin deficient curled root phenotype (Fig. 1B). In contrast, PISA did not rescue
165 these root defects caused by auxin deficiency, clearly indicating PISA does not directly act as a
166 typical auxin like IAA or NAA in planta (Fig. 1B and S1A).

167 The tobacco BY-2 cell suspension culture requires auxin for cell proliferation (Winicur et al.,
168 1998). BY-2 cells proliferated in the presence of IAA and NAA (Fig. S1B), but PISA failed to maintain
169 this cell culture (Fig. S1B). The cell morphology of the culture treated with PISA showed swollen cell
170 shapes that are a hallmark of auxin-depletion (Fig. S1C) further suggesting that PISA does not act as
171 an auxin on cell division (Winicur et al., 1998). Auxin-induced rapid cell elongation in etiolated
172 hypocotyls was demonstrated to be mediated by TR1/AFB receptors (Fendrych et al., 2016).
173 However, PISA failed to induce this rapid cell elongation (Fig. S2), suggesting that PISA does not act
174 as a conventional auxin to directly activate the TR1/AFB receptors in the hypocotyl.

175 IAA and the synthetic auxin picloram cause potent induction of auxin-responsive reporter genes
176 such as *DR5* (Fig. 1C). In contrast, PISA did not induce any auxin-responsive *DR5::GUS* and
177 *BA3::GUS* reporter expression, again suggesting that it is inactive as a ligand for the $SCF^{TIR1/AFB}$
178 pathway (Fig. 1C, 1D and S3A). DII-VENUS protein is a translational fusion of the TIR1-interacting
179 domain of Aux/IAA proteins and the fluorescent reporter VENUS (Brunoud et al., 2012). IAA
180 promotes the interaction between DII-VENUS and TIR1 receptor to induce the DII-VENUS
181 degradation and loss of the VENUS signal (Fig. 1E). In contrast, PISA did not induce degradation of
182 DII-VENUS, once again suggesting that PISA does not directly modulate TIR1/AFB-Aux/IAA auxin
183 co-receptor complex formation. Additionally, PISA showed no activity in the yeast auxin-inducible

degron (AID) system (Fig. S3B) (Nishimura et al., 2009). In this system, the minichromosome maintenance (MCM) complex is essential for DNA replication in yeast and lines in which MCM is deficient fail to grow (Nishimura et al., 2009). The auxins IAA and NAA, and analog mPISA, all repressed the growth of yeast expressing rice OsTIR1 and Aux/IAA-fused MCM4 protein by promoting the degradation of the fused MCM4 protein (Fig. S3B) (Nishimura et al., 2009). In contrast, PISA did not repress yeast growth in this AID system, indicating again that PISA is not an active ligand for TIR1.

These findings were further supported by biochemical assays using Surface Plasmon Resonance (SPR) analysis (Fig. 1F) and a pull-down assay (Fig. S3C) (Lee et al., 2014). IAA promotes assembly of the co-receptor complex of TIR1 and Aux/IAA (domain II) in both assays. In contrast, PISA did not promote the interaction between TIR1 and Aux/IAA in either system (Fig. 1F and S3C). Additionally, the SPR assay also showed that there was no binding of PISA with AFB5 (Fig. S3D), and using the SPR assay to test for anti-auxin activity by mixing 50 μM PISA with 5 μM IAA showed that PISA did not bind and block the TIR1 auxin-binding site (Fig. S3E) whereas the known TIR1/AFB auxin receptor blocker auxinole (Hayashi et al., 2012) reduced the IAA signal dramatically. Thus, in these direct binding assays, PISA does not bind to TIR1/AFB co-receptors. In summary, PISA is completely inactive as a classical auxin that induces the Aux/IAA degradation via TIR1/AFB auxin receptors.

PISA promotes hypocotyl elongation by positively modulating polar auxin transport.

PISA promotes hypocotyl elongation in a manner that is typical for auxin effects in Arabidopsis seedlings (Fig. 2A). Since PISA did not activate DR5-monitored auxin response, we carefully examined its effects on auxin-related phenotypes *in planta* in order to address possible modes of PISA action. In light-grown seedlings, PISA at 5 - 20 μM promoted hypocotyl elongation (Fig. 2A-2D). In contrast, IAA and mPISA inhibited growth at 0.5 and 20 μM, respectively, whereas the AFB5-selective synthetic auxin picloram strongly promoted hypocotyl elongation (Fig. 2D). In the

dark, PISA at 2 μM slightly promoted the elongation of etiolated hypocotyls (Fig. 2E and 2F), but did not inhibit the elongation at 20 μM. In contrast, exogenously applied IAA, picloram and mPISA inhibited the elongation of etiolated hypocotyls (Fig. 2F).

Having explored a set of physiological responses, we made use of genetic and pharmacological tools to gain insight into the mechanism of PISA action. The auxin signaling mutants *axr1-3* and *tir1-1 afb2-1* showed high resistance to mPISA (Fig. S4A), implying mPISA targets auxin signaling in planta (Hayashi, 2012). In contrast, the hypocotyl of *axr1-3* elongated to a similar extent as wild type when treated with PISA (Fig. 3A). Importantly, neither wild-type nor *axr1-3* responded to PISA after the inhibition of SCF^{TIR1} auxin signaling by the auxin antagonist auxinole (Fig. 3A and S4B). PISA also failed to promote hypocotyl elongation in the presence of the auxin biosynthesis inhibitor L-kynurenine (Fig. 3A and S4C). These observations indicate that auxin-like effects of PISA on hypocotyl growth require the $SCF^{TIR1/AFB}$ auxin signaling to be activated by endogenous IAA.

To examine the effects of PISA on polar auxin transport, seedlings were co-treated with auxin efflux transport inhibitors and PISA. The promotion of elongation by PISA on hypocotyls was blocked by three auxin efflux transport inhibitors, TIBA, BUM (2-[4-(diethylamino)-2-hydroxybenzoyl]benzoic acid) and NPA (Fig. 3B, 3C and S5A) (Fukui and Hayashi, 2018). In addition, treatments with the synthetic auxin picloram and the auxin overproduction line *35S::YUC1* exhibited longer hypocotyls as a high auxin phenotype (Fig. S5B), but in these lines TIBA and NPA did not suppress the elongation (Fig. S5B). The data suggest that PISA could positively modulate polar auxin transport in hypocotyls. To examine further the effects of PISA on basipetal auxin transport, rootward movement of ^{3}H-IAA was analyzed (Fig. 3E). In this assay, NPA reduced the basipetal movement of ^{3}H-IAA in hypocotyls, whereas PISA enhanced it (Fig. 3E). These results collectively show that PISA positively modulates basipetal auxin transport in hypocotyls. Another possible target of PISA could be the regulation of endogenous auxin concentrations, such as via auxin biosynthesis or catabolism. Analysis of endogenous IAA levels in Arabidopsis seedlings showed that they were not affected by PISA treatment (Fig. S6). Together, these results indicate that PISA likely acts by affecting polar

auxin transport.

PISA inhibits root growth by accumulating IAA at the root tip.

PISA inhibited primary root growth in a manner that is similar to conventional auxins. The seedlings were cultured on vertical plates containing PISA for 7 days (Fig. 4A-4C). The auxin signaling mutants, *axr1-3* and *tir1 afb2* were insensitive to PISA. Additionally, auxin influx transport mutant *aux1-7* was also less sensitive to PISA in root growth (Fig. 4C). Taken together with the effects of PISA on auxin transport in the hypocotyl, these results suggest that PISA inhibits primary root growth by modulating auxin transport to affect auxin distribution and maxima. Further, the roots treated with PISA at 100 μM showed severe defects in root cell morphology (Fig. 4B). To examine the effects of PISA on auxin distribution in root, *DR5::GFP* seedlings were cultured with PISA for 7days (Fig. 4D). PISA significantly induced GFP expression in the lateral root cap cell, indicating PISA accumulates IAA in the lateral root cap and root growth is inhibited as a consequence. In contrast to auxin signaling mutants, the sensitivity of *pin2* and *pin3 pin7* mutants was comparable to wild-type (Fig. 4C). To investigate the short-term effects of PISA, seedlings were treated with PISA for 5 h (Fig. 4E). PISA inhibited root elongation within this 5 h incubation. The *tir1 afb2* mutant was insensitive to PISA, but the *pin2* mutant was more sensitive to PISA than WT. Perhaps, in the *pin 2* mutant, the accumulated IAA is not efficiently transported from the lateral root cap. Consistent with root elongation responses (Fig. 4E), PISA induced *DR5::GFP* expression in the lateral root cap after 20h treatment suggesting enhanced accumulation of endogenous IAA (Fig. 4F). The auxin transport inhibitor TIBA blocks IAA efflux and inhibits root elongation by accumulating IAA (Fig. S5). TIBA highly induced *DR5::GFP* expression near the quiescent center where IAA is biosynthesized (Fig. 4F) (Brumos et al., 2018). Taken together, these results indicate that PISA promotes the auxin transport rate leading to accumulations of IAA at the lateral root cap, resulting in the inhibition of root elongation.

PISA blocked root hair formation by positively modulating auxin transport.

PISA displayed auxin-like activity in hypocotyl elongation, primary root inhibition and adventitious root formation (Fig. 2). Typical auxin efflux transport inhibitors commonly inhibit the elongation of both primary root and hypocotyl, supporting PISA is not an inhibitors of auxin efflux transport. The effects of PISA on auxin-related phenotypes can be explained if it works by increasing auxin efflux. To further examine the effects of PISA on auxin efflux transport, the root hair phenotype was analyzed. This process involves the PIN2 proteins, which are localized at apical side of root epidermal cells and mainly contribute to basipetal (shootward) auxin transport (Abas et al., 2006). The loss of function *pin2/eir1* mutant displays impaired root hair formation (Fig. 5A and 5B). The ectopic overexpression of PIN1 in *35S::PIN1* roots also interferes with this shootward auxin transport, consequently, *35S::PIN1* seedlings also show defects in root hair formation (Fig. 5A and 5B) (Ganguly et al., 2010), suggesting shootward auxin flow is important for root hair formation (Rigas et al., 2013). In contrast, auxin efflux transport inhibitors TIBA and NPA promote root hair formation (Ganguly et al., 2010), probably by increasing the accumulation of endogenous IAA (Fig. 5C). Importantly, PISA inhibits root hair formation, implying PISA has an opposite effects to auxin efflux inhibitors.

PISA affects adventitious and lateral root formation by positively modulating auxin transport

PISA induces adventitious root formation at the shoot/root junction as shown in Fig. 2A. Importantly, auxin signaling mutants *slr/iaa14* and *arf7 arf19* show severe defects in lateral root formation (Fig. 3D and table 1) (Okushima et al., 2007). In these mutants PISA did not promote adventitious root formation at shoot/root junction and this is consistent with the auxin-like effects of PISA on hypocotyls (Fig. 3D and table 1). This suggests that adventitious root formation in response to PISA treatment depends on auxin signaling downstream of $SCF^{TIR1/AFB}$. In such a situation, auxin efflux transport inhibitors BUM, NPA and TIBA would reduce polar auxin transport in hypocotyls, resulting in the inhibition of the adventitious root formation and this is indeed what we observed, as shown in Table 1 and Fig. S5A. Taken together, these results suggest that PISA positively modulates the polar

auxin transport system, thereby leading to the accumulation of auxin at the shoot/root junction and promoting adventitious root formation.

In contrast to the promotion of adventitious roots at the shoot/root junction (Table 1 and Fig. 2A), PISA alone repressed lateral root formation in primary roots (Fig. 6A). In contrast, PISA strongly promoted lateral root numbers when co-incubated with exogenous IAA (Fig. 6B, 6C and S7A). TIBA and NPA did not affect the lateral root number induced by exogenous IAA (Fig. S8A), suggesting that inhibition of auxin efflux does not enhance IAA-induced lateral root formation. This was further investigated using the cell cycle reporter *CYCB1;1::GUS,* which is induced strongly by IAA and NAA in initiating lateral roots. In this assay, PISA enhanced *CYCB1;1::GUS* expression when in the presence of auxins, IAA and NAA (Fig. S7B). Similarly, auxin-induced *DR5::GUS* expression was dramatically enhanced by pretreatments with PISA (12 h) (Fig. 6D). In this experiment, IAA treatment for 6h at 100 and 500 nM induced *DR5::GUS* expression in elongation zones only (Fig. 6D). This expression pattern was extended along the entire root by the co-incubation of IAA and PISA (Fig. S8B). In contrast, co-treatment with IAA and auxin transport inhibitors (NPA, TIBA, Bz-IAA (5-benzykoxy IAA) and BUM) (Fukui and Hayashi, 2018) activated *DR5::GUS* expression only at the root tips (Fig. 6D). To examine the effects of PISA on basipetal auxin transport, shootward movement of IAA from the root tip was evaluated by *DR5::GUS* assay (Fig. 6E) (Buer and Muday, 2004; Lewis and Muday, 2009). In this shootward auxin transport assay, the *DR5::GUS* seedlings were placed on vertical plate containing PISA and then an agar block containing IAA was placed onto the root tips. The seedlings were then incubated for 10 h. PISA promoted *DR5::GUS* induction derived from root tip IAA (Fig. 6E), suggesting PISA enhances shootward auxin transport from the root tip. Taken together, these results indicate that PISA increases the net flow of auxin in the roots by positively modulating auxin transport.

Other possible targets for PISA are the AUX1/LAX auxin influx transporters. PISA might promote IAA-induced lateral root formation by increasing the uptake of exogenous IAA. To test the effects of PISA on IAA influx transport, seedlings were co-treated with PISA and membrane permeable IAA

prodrugs, IAA methyl ester and IAA octyl ester (Fig. S9). These lipophilic IAA esters and NAA (Fig. S7B) can be incorporated into cells by passive diffusion, but not by the AUX1/LAX transporters. PISA enhanced lateral root formation to the same extent with the two IAA esters, NAA and IAA (Fig. S7B and S9), indicating IAA influx transport was not required for the activity of PISA on lateral root promotion.

PISA perturbed asymmetric auxin distribution and gravitropism in root.

Gravistimulation rapidly induces asymmetric auxin distributions in roots and thereby changes the *DR5* reporter expression pattern (Fig.7A). This gravistimulated asymmetric auxin distribution is driven by PIN-mediated shootward auxin movement in the root epidermis (Wisniewska et al., 2006; Baster et al., 2013). After 4h gravistimulation, the *DR5::GFP* signal increased at the lower side of gravistimulated roots. PISA treatment completely diminished this asymmetric expression of *DR5::GFP* (Fig.7A and 7B) and concomitantly blocked root gravitropic responses (Fig. 7C). These observations show that PISA not only modulates polar auxin transport but specifically affects PIN-mediated asymmetric auxin distribution in gravistimulated roots.

PISA blocked the internalization of PIN proteins and promoted their accumulation at the plasma membrane.

All the phenotypic effects of PISA can be explained by the positive modulation of auxin transport by PISA. PISA treatment did not affect the expression profiles of *proPIN1::GFP*, *proPIN2::GUS* and *proPIN7::GUS* (Fig. S10), indicating that the primary target of PISA in auxin transport is not the regulation of PIN transcription. To address the mechanism of positive effects of PISA on auxin efflux, we examined the effects of PISA on the recycling of PIN proteins in roots. Brefeldin A (BFA) induces the formation of BFA bodies which incorporate PIN2-GFP protein in *proPIN2::PIN2-GFP* line (Geldner et al., 2003). Auxin (NAA) was shown to inhibit BFA body formation by blocking the endocytosis of PIN2 protein (Fig. 8A) (Paciorek et al., 2005). The negative control compound

benzoic acid did not affect BFA body formation (Fig. 8A), but PISA inhibited BFA body formation in the same extend as NAA (Fig. 8A and 8B). Additionally, BFA body formation with both PIN1-GFP fusion and PIN1 native protein, was also blocked by NAA and PISA (Fig. S11). These observations suggest that PISA interferes with PIN recycling or vacuolar targeting, and as a consequence promotes the accumulation of PIN proteins at the PM. Since constitutive PIN recycling has been linked to maintenance of its asymmetric, polar distribution, we tested PISA effect on PIN polarity. Indeed, PISA treatment diminished PIN2 polarity at the PM. PIN2 showed pronounced accumulation at the lateral cell sides (Fig. 8C, 8D and S12) and PIN1 showed almost no polarity after treatment with PISA (Fig. S13). Furthermore, PISA at 100 µM disrupted the root architectures and PIN2 polar localization (Fig. S14).

This change in the localization of PIN proteins was further investigated using PINOID (PID), a serine threonine kinase of the AGC kinase family which is known to regulate PIN localization on the cellular membranes (Adamowski and Friml, 2015). Overexpression of PID triggers a basal to apical shift in PIN1 localization, thereby perturbing the auxin gradient in the root tip; depleting auxin from the root tip maxima and leading to meristem collapse (Benjamins et al., 2001; Friml et al., 2004). Consistently, PIN1 was localized at apical side in the endodermis of *35S::PID* roots (Fig. 8F). Intriguingly, PISA rescued collapsed root meristems in *35S::PID* roots (Fig. 8E) and the typical apical polarity of PIN1 in *35S::PID* was lost and switched to an apolar pattern in endodermal cells (Fig. 8F). Thus, PISA appears to repress IAA depletion from the *35S::PID* apical meristem by diminishing shootward IAA transport. This is fully consistent with the PISA effect on the polar localization of PIN proteins.

To gain further insight into the mechanism by which PISA induces PIN accumulation at the PM, the effects of PISA on PIN2-GFP accumulation were examined in a *tir1 afb1 afb2 afb3* quadruple mutant line (Fig. S15). As in WT roots, PIN2-GFP protein was found to be predominantly apical and not lateral cell sides despite the severe growth defects in these roots. PISA promoted the accumulation of PIN2-GFP at lateral cell sides in the quadruple mutant, the same as in the wild type

366 root. This observation strongly suggests that PISA leads to increases in PIN protein accumulation at
367 the PM without activating the $SCF^{TIR1/AFB}$ pathway.
368
369 **DISCUSSION**
370 **Pinstatic acid is an inert for the TIR1/AFB-Aux/IAA co-receptor complex**
371 In the screening for the auxin transport modulators from the PAA analogs, pinstatic acid
372 (4-ethoxyphenylacetic acid: PISA) was found to be the most promising candidate. PISA does not
373 bind to the $SCF^{TIR1/AFB}$ complex. The classical structure activity relationships of mono-substituted
374 phenylacetic acids demonstrated that 4-substituted PAA is less or inactive as an auxin (Muir et al.,
375 1967). Consistent with these early structure activity relationship studies of PAA derivatives, our
376 results clearly demonstrated that PISA is not a classical auxin directly modulating the $SCF^{TIR1/AFB}$
377 machinery (Fig. 1). Consistent with this, a docking study using the auxin binding cavity of TIR1
378 showed that the 4-ethoxy chain in PISA would prevent stable binding of this compound (Fig. S16).
379 In analogy to PISA, the introduction of alkyloxy chains into IAA and NAA at the 5- or
380 6-positions diminished their TIR1 binding activity (Tsuda et al., 2011). However, it appears that these
381 alkoxy-IAA and -NAAs are still recognized by PIN efflux proteins to inhibit polar IAA transport in
382 competition with endogenous IAA (Tsuda et al., 2011), suggesting alkoxy-IAAs and alkoxy-NAAs
383 could act as auxin transport inhibitors. On the other hand, PAA is not actively and directionally
384 transported in response to gravitropic stimuli and the distribution of PAA is not inhibited by NPA,
385 suggesting that PAA is distributed by passive diffusion (Sugawara et al., 2015). As for PAA, it seems
386 unlikely that PISA itself would be recognized by PINs in planta.
387
388 **PISA positively modulates polar auxin transport to induce auxin-like activity.**
389 PISA showed characteristic auxin-like activity on primary root and shoot responses. PISA inhibited
390 primary root elongation and induced adventitious root formation at the shoot / root junction (Fig. 2).
391 The auxin signaling mutants *axr1-3*, *tir1 afb2*, *slr1-1* and *arf7 arf19* were resistant to PISA in primary

root inhibition and adventitious root formation, suggesting that some PISA-induced responses might be mediated by the $SCF^{TIR1/AFB}$ signaling pathway (Fig. 4D). However, these responses can also be well explained by the accumulation of endogenous IAA at root tip and the shoot / root junction following elevated IAA efflux. Auxin efflux inhibitors completely repressed adventitious root formation induced by PISA (Table 1), suggesting that IAA movement is required for PISA activity on adventitious root formation. In the primary root, IAA is biosynthesized near the quiescent center (QC) where TAA1 is strongly expressed (Brumos et al., 2018). Auxin efflux inhibitors, TIBA and NPA are considered to have repressed IAA efflux leading to induction of *DR5::GFP* expression near the QC (Fig. 4D) and then results in the inhibition of root elongation (Brumos et al., 2018). In contrast, PISA would promote auxin efflux from the QC to lateral root cap, thereby *DR5::GFP* signal was induced at that place (Fig. 4D). Thus, PISA inhibits root elongation by distinct mechanism of auxin efflux inhibitors.

Furthermore, PISA promoted hypocotyl elongation. Auxin efflux transport inhibitors, TIBA, NPA and BUM completely suppressed hypocotyl elongation (Fig. 3B, 3C and S5A). Hypocotyl elongation by synthetic auxin picloram or YUC1 overexpression could not be cancelled by auxin efflux transport inhibitors (Fig. S5B). These evidences suggest that PISA positively modulated auxin transport to show auxin-like activity in the hypocotyl. This was further confirmed by ^{3}H-IAA transport assays in hypocotyl segments (Fig. 3E). Importantly, no auxin analog has been reported to be positive modulator of auxin transport.

PISA affects root auxin responses by positively modulating shootward auxin transport.

In contrast to auxin-like effects on primary root growth and shoot elongation, PISA-treated roots showed typical auxin-repressed phenotypes: reduced root hair formation, fewer lateral roots and reduced gravitropic response. Auxin transport inhibitors promoted root hair formation (Fig. 5B) by accumulating endogenous IAA, but blocked lateral root formation and gravitropic responses by perturbing auxin distribution. The impaired root phenotypes by PISA resemble the root defects in

PIN1 overexpressing roots (Rigas et al., 2013), supporting the hypothesis that PISA represses auxin-regulated phenotypes by enhancing auxin efflux. Intriguingly, PISA dramatically enhanced IAA-induced lateral root formation and PISA also promoted IAA-induced *DR5::GUS* expression in entire roots when auxin transport inhibitors did not (Fig. 6B – 6D). Additionally, PISA enhanced shootward auxin movement from the root tip in basipetal auxin transport assays (Fig. 6E). PISA did not increase the endogenous IAA (Fig. S6). Thus, it is unlikely that PISA would elevate endogenous IAA in the shoot by up-regulating *TAA1* and *YUC* expression in the IAA biosynthesis pathway or by inhibiting the IAA inactivation pathway involving GH3 and DAO1 (Korasick et al., 2013). These observations suggest that PISA positively modulates shootward IAA transport in the root.

PISA blocks PIN internalization to accumulate PIN at plasma membrane in Arabidopsis.

The localization and trafficking of PIN1 and PIN2 proteins have been extensively investigated (Adamowski and Friml, 2015; Rakusova et al., 2015). ROP GTPases-RIC signaling have been shown to inhibit the PIN internalization (Lin et al., 2012; Nagawa et al., 2012), PINOID kinase and D6 Protein Kinase could directly phosphorylate PIN at the PM to regulate the PIN trafficking in a GNOM dependent manner (Adamowski and Friml, 2015). However, the molecular mechanism for the regulation of PIN trafficking, especially PIN internalization, by auxin has been unclear. Our results show that PISA inhibited the formation of BFA bodies containing PIN1 and PIN2 proteins (Fig. 8, and S11). Furthermore, PISA promoted the accumulation of PIN1 and PIN2 proteins at the lateral side of cells. These observations, together with phenotypic data, clearly indicate that by inhibiting PIN internalization PISA would increase PM-localized PIN content, leading to characteristic phenotypes caused by enhanced auxin efflux.

The target of PISA remains an open and intriguing question. PISA is completely inert for transcriptional auxin signaling modulated by SCF $^{TIR1/AFB}$ –Aux/IAA machinery. PISA enhanced PIN2 accumulation at the PM in *tir1 afb1 afb2 afb3* quadruple mutant (Fig. S15) (Pan et al., 2009), implying TIR1/AFB receptors are not a prerequisite for the inhibition of PIN2 internalization by PISA.

Modulation of PIN localization and trafficking are influenced by many regulatory steps (Adamowski and Friml, 2015) and it is likely that auxin could coordinately modulate pathways involving recycling rate, biosynthesis and degradation of PINs in response to environmental and hormonal stimuli.

Many questions still remain as to the mode of action of PISA. It has been reported that auxin reduced formation of BFA bodies by inhibiting delivery of newly synthesized protein rather than by inhibition of PIN internalization (Jasik et al., 2016). On the other hand, PISA inhibited BFA body formation of PIN2-GFP, but enhanced amounts of PIN2-GFP on the PM suggesting that delivery is not impaired and internalization is reduced. Given this, we have no reason to believe that PISA would target the regulatory component of PIN internalization to which endogenous auxin would bind. We anticipated that PISA will be a very useful chemical tool to dissect the regulatory mechanism of auxin transport.

MATERIALS AND METHODS

Plant materials and growth conditions

Arabidopsis (*Arabidopsis thaliana*) ecotype Columbia (Col-0) was used for all experiments. The following transgenic and mutant lines were in the Col-0 ecotype: *axr1-3* [CS3075], *tir1-1 afb2-3* [CS69691], *iaa14/slr1-1* (Okushima et al., 2007; Spartz et al., 2012; Chae et al., 2012), *arf7 arf19* (Okushima et al., 2007), *DII-VENUS* (Brunoud et al., 2012), *yuc3 5 7 8 9* (Chen et al., 2014), *proPIN1::PIN1-GFP* (Vieten et al., 2005), *proPIN2::PIN2-GFP* (Vieten et al., 2005), *pin2/eir1-1* [CS16706], *35S::PIN1* [CS9375], *35S::PID* (Benjamins et al., 2001), *pPIN2::PIN2-GFP / tir1 afb1 afb2 afb3* (Pan et al., 2009). Seeds were surface-sterilized and grown on germination medium (GM; 0.5× Murashige and Skoog salts [Gibco-BRL], 1% Suc, 1× B5 vitamins, and 0.2 g/L MES containing 1.2% sucrose and 4 g/L agar for horizontal agar plate or 14 g/L agar for vertical agar plates, pH 5.8) containing the indicated hormone and/or chemicals. The length of hypocotyl and lateral root number was measured using ImageJ software.

Chemicals

4-ethoxyphenylacetic acid [CAS Registry Number: 4919-33-9], PISA and 3-ethoxy-phenylacetic acid, mPISA was synthesized from 4-hydroxyphenylacetic acid methyl ester and 3-hydroxyphenylacetic acid methyl ester, respectively. PISA is commercially available from some chemical suppliers (Alfa Aesar, Santa Cruz Biotechnology and, ACROS ORGANICS).

Histochemical and Quantitative GUS Measurements

For GUS histochemical analysis, the seedlings were washed with a GUS-staining buffer (100 mm sodium phosphate, pH 7.0, 10 mM EDTA, 0.5 mMm $K_4Fe(CN)_6$, 0.5 mM $K_3Fe(CN)_6$, and 0.1% Triton X-100) and transferred to the GUS-staining buffer containing 1mM 5-bromo-4-chloro-3-indolyl-β-d-glucuronide (X-Gluc), the substrate for histochemical staining, and incubated at 37°C until sufficient staining developed. For quantitative measurement, seedlings or the excised roots (n = 15–20) were homogenized in an extraction buffer as described previously (Hayashi et al., 2012). After centrifugation to remove cell debris, GUS activity was measured with 1 mM 4-methyl umbelliferyl-β-d-glucuronide as a fluorogenic substrate at 37°C. The protein concentration was determined by Bradford protein assay (Bio-Rad). The experiments were repeated at least three times with four replications.

DII-VENUS assay

6-d-old DII-VENUS seedlings (Brunoud et al., 2012) were incubated in GM liquid medium containing 10 μM yucasin DF for 3h at 24°C. The DII-VENUS seedlings were washed out well with fresh medium and incubated in fresh GM liquid medium for 5 min. Exogenous IAA and PISA was added to this medium and fluorescent images of roots were recorded after 60 min.

Surface plasmon resonance assay:

Surface plasmon resonance assays were performed as described previously (Quareshy et al.,

2017). 50 µM IAA or PISA were used to assay for the formation of the auxin-induced TIR1 - IAA7 co-receptor complex, or AFB5 - IAA7 complex. For the anti-auxin assay, 5 µM IAA and 50 µM PISA (or control compound) were mixed and the sensorgram assessed for a reduced signal to the IAA.

Exogenous IAA-induced lateral root promotion

For lateral root growth, Arabidopsis seedlings were grown vertically for 5 d in continuous light on GM agar plate. The seedlings were transferred to liquid GM medium containing the indicated concentration of IAA and PISA. The seedlings were cultivated under continuous light for another 3 d at 24°C and then the lateral root numbers were recorded. Three independent experiments were performed.

Gravitropic response assay

6-d-old seedlings were grown vertically on GM agar plates under continuous light at 24°C. The seedlings were then transferred to agar plates containing chemicals and cultured vertically for 2 h. The plates were rotated 90° in the vertical plane, followed by incubation for 16 h in the dark. Photographs of the roots were recorded with a digital camera.

Auxin transport assay

For shoot basipetal transport, 6-d-old Col-0 etiolated seedlings grown on GM agar plates were decapitated to avoid endogenous auxin biosynthesis in cotyledons and a droplet of GM agar (1.25 %) with ^{3}H-IAA was applied to apical part of the hypocotyls. The seedlings were preincubated with 20 µM PISA for 1 h on agar plate containing PISA. After 6 hours, all roots were removed, hypocotyls were collected, homogenized using grinder and liquid nitrogen and incubated overnight in Opti-Fluor scintillation solution (Perkin Elmer). The amount of ^{3}H-IAA was measured in a scintillation counter (Hidex 300SL) for 300s with three technical repetitions. The decapitated seedlings were placed on GM agar plate containing 5 µM NPA to inhibit auxin transport, and then ^{3}H-IAA agar droplet

was applied to apical part. The negative control (diffusion) was estimated with seedlings transferred to GM agar containing 5 μM NPA during the ^{3}H-IAA droplets incubation (6 h) to inhibit auxin transport.

The root basipetal transport assay was carried out with slight modifications according to the method of D.R. Lewis (Lewis and Muday, 2009). A narrow strip of aluminum foil was vertically embedded in GM agar plate (2.0 %) containing 40 μM PISA. 5-d-old *DR5::GUS* seedlings were placed on the GM agar so that the root tip stepped over the edge of the foil strip. An agar block (10 μM IAA and 40 μM PISA) was placed on the root tip. The aluminum strip blocks the diffusion of IAA into the GM agar plate. The plate was incubated vertically for 10 h and GUS activity was visualized histochemically with X-Gluc.

Asymmetric auxin distribution measurement and PIN immunolocalization analysis

All measurements were performed using ImageJ software (National Institutes of Health; http://rsb.info.nih.gov/ij). Quantification of auxin asymmetry was performed on maximal intensity projection of Z-scans of root tip by measuring ratio of signal intensity of upper/lower half of the root. *DR5rev-GFP* reporter line was imaged before and after gravistimulation. PIN immunolocalizations of primary roots were carried out as described (Sauer et al., 2006; Robert et al., 2010). The antibodies used in this study were as follows: anti-PIN1, 1:1000 and anti-PIN2, 1:1000.

Imaging and Image Analysis.

Fluorescence images were recorded with a fluorescence microscope (Olympus; BX-50) and a laser scanning confocal microscope (Olympus; FV-3000). Typically, the seedlings were incubated with half-strength MS medium containing chemcials for the indicated time at 24 °C and fluorescence images were then immediately recorded. For quantification of the fluorescent signal in epidermal cell in *proPIN2::PIN2-GFP* and *proPIN1::PIN1-GFP*. The same image acquisition parameters were used for all signal measurements. the regions of the visible BFA bodies in the same number and area of root cell were selected and the BFA body signal area (the area of BFA body / the constant root cell

548 area containing same cell number) were calculated by image J software. To measure signal intensity
549 of PM-localized PIN2-GFP, the mean pixel intensities were obtained from the apical and lateral sides
550 of the individual cells by Image J software. The PM-accumulation of PIN2-GFP was shown as the
551 ratio of intensity (the apical side / the lateral side), 50-60 cells were analyzed for 5-7 seedlings in
552 three independent treatments.
553
554 **Statistical Analysis**
555 Statistically significant differences in the results (**$P < 0.05$ or *$P < 0.01$) are based on Welch's
556 two sample t-test by SigmaPlot 14.0. The values of mock-treated and PISA-treated samples (Fig. 2,
557 3, 5, 6, 7, and 8) and the values of wild-type and mutants treated with PISA at same concentration
558 (Fig. 4) were statistically tested. Data are means ± SD of independent replicates. Box-and-whisker
559 plots show a median (centerline), upper/lower quartiles (box limits) and maximum/minimum
560 (whiskers).
561
562 **Supplemental Data**
563 The following supplemental materials are available.
564 Supplemental Figure S1. Auxin activity in an auxin-deficient Arabidopsis mutant and BY2 tobacco
565 cell culture.
566 Supplemental Figure S2. Effects of PISA on rapid cell expansion in hypocotyl.
567 Supplemental Figure S3. Effects of PISA on SCF^{TIR1} signaling.
568 Supplemental Figure S4. Effects of mPISA and PISA on the phenotype related to $SCF^{TIR1/AFB}$
569 pathway.
570 Supplemental Figure S5. Auxin transport inhibitors blocked PISA-induced high-auxin phenotype, but
571 did not inhibit the high-auxin phenotypes by picloram and YUC1 overexpression.
572 Supplemental Figure S6. Effects of PISA on endogenous IAA level.

Supplemental Figure S7. Phenotype of Arabidopsis seedlings co-cultured with PISA and auxins.

Supplemental Figure S8. Effects of PISA and auxin transport inhibitors on auxin response in root.

Supplemental Figure S9. PISA promoted the lateral root formation induced by membrane permeable IAA precursors.

Supplemental Figure S10. PISA did not affect the expression of *PIN1::GUS*, *PIN2::GUS* and *PIN7::GUS* reporter expression.

Supplemental Figure S11. Effect of PISA on the BFA body formation of PIN1.

Supplemental Figure S12. Effect of PISA on the internalization of PIN2-GFP.

Supplemental Figure S13. Effect of PISA on the internalization of PIN1.

Supplemental Figure S14. Effect of PISA on the internalization of PIN2 at high concentration.

Supplemental Figure S15. Effects of PISA on PIN2 membrane localization in *tir1 afb 1 afb 2 afb3* mutant.

Supplemental Figure S16. Molecular docking study of PAA, mPISA and PISA with TIR1.

ACKNOWLEDGEMENTS

We thank Dr. H. Fukaki (University of Kobe), Dr. R. Offringa (Leiden University), Dr. Jianwei Pan (Zhejiang Normal University) and Dr. M. Estelle (University of California at San Diego) for providing mutants and transgenic line seeds. The research leading to these results has received funding from JSPS KAKENHI (Grant Number JP25114518) to K.H. and European Union's Horizon2020 program (ERC grant agreement n° 742985) to J.F.

LITERATURE CITED

Abas L, Benjamins R, Malenica N, Paciorek T, Wisniewska J, Moulinier-Anzola JC, Sieberer T, Friml J, Luschnig C (2006) Intracellular trafficking and proteolysis of the Arabidopsis auxin-efflux facilitator PIN2 are involved in root gravitropism. Nat Cell Biol **8:** 249-256

Adamowski M, Friml J (2015) PIN-dependent auxin transport: action, regulation, and evolution. Plant Cell **27:** 20-32

Adamowski M, Narasimhan M, Kania U, Glanc M, De Jaeger G, Friml J (2018) A Functional Study of AUXILIN-LIKE1 and 2, Two Putative Clathrin Uncoating Factors in Arabidopsis. Plant Cell **30:** 700-716

Baster P, Robert S, Kleine-Vehn J, Vanneste S, Kania U, Grunewald W, De Rybel B, Beeckman T, Friml J (2013) SCF(TIR1/AFB)-auxin signalling regulates PIN vacuolar trafficking and auxin fluxes during root gravitropism. EMBO J **32:** 260-274

Benjamins R, Quint A, Weijers D, Hooykaas P, Offringa R (2001) The PINOID protein kinase regulates organ development in Arabidopsis by enhancing polar auxin transport. Development **128:** 4057-4067

Brumos J, Robles LM, Yun J, Vu TC, Jackson S, Alonso JM, Stepanova AN (2018) Local Auxin Biosynthesis Is a Key Regulator of Plant Development. Dev Cell **47:** 306-318 e305

Brunoud G, Wells DM, Oliva M, Larrieu A, Mirabet V, Burrow AH, Beeckman T, Kepinski S, Traas J, Bennett MJ, Vernoux T (2012) A novel sensor to map auxin response and distribution at high spatio-temporal resolution. Nature **482:** 103-106

Buer CS, Muday GK (2004) The transparent testa4 mutation prevents flavonoid synthesis and alters auxin transport and the response of Arabidopsis roots to gravity and light. Plant Cell **16:** 1191-1205

Chae K, Isaacs CG, Reeves PH, Maloney GS, Muday GK, Nagpal P, Reed JW (2012) Arabidopsis SMALL AUXIN UP RNA63 promotes hypocotyl and stamen filament elongation. Plant J **71:** 684-697

Chen Q, Dai X, De-Paoli H, Cheng Y, Takebayashi Y, Kasahara H, Kamiya Y, Zhao Y (2014) Auxin overproduction in shoots cannot rescue auxin deficiencies in Arabidopsis roots. Plant Cell Physiol **55:** 1072-1079

Ding Z, Galvan-Ampudia CS, Demarsy E, Langowski L, Kleine-Vehn J, Fan Y, Morita MT, Tasaka M, Fankhauser C, Offringa R, Friml J (2011) Light-mediated polarization of the PIN3 auxin transporter for the phototropic response in Arabidopsis. Nat Cell Biol **13:** 447-452

Du Y, Tejos R, Beck M, Himschoot E, Li H, Robatzek S, Vanneste S, Friml J (2013) Salicylic acid interferes with clathrin-mediated endocytic protein trafficking. Proc Natl Acad Sci U S A **110:** 7946-7951

Fendrych M, Leung J, Friml J (2016) TIR1/AFB-Aux/IAA auxin perception mediates rapid cell wall acidification and growth of Arabidopsis hypocotyls. Elife **5**

Friml J, Yang X, Michniewicz M, Weijers D, Quint A, Tietz O, Benjamins R, Ouwerkerk PB, Ljung K, Sandberg G, Hooykaas PJ, Palme K, Offringa R (2004) A PINOID-dependent binary switch in apical-basal PIN polar targeting directs auxin efflux. Science **306:** 862-865

Fukui K, Hayashi KI (2018) Manipulation and Sensing of auxin metabolism, transport and signaling. Plant Cell Physiol

Furutani M, Nakano Y, Tasaka M (2014) MAB4-induced auxin sink generates local auxin gradients in Arabidopsis organ formation. Proc Natl Acad Sci U S A **111:** 1198-1203

Ganguly A, Lee SH, Cho M, Lee OR, Yoo H, Cho HT (2010) Differential auxin-transporting activities of PIN-FORMED proteins in Arabidopsis root hair cells. Plant Physiol **153:** 1046-1061

Geldner N, Anders N, Wolters H, Keicher J, Kornberger W, Muller P, Delbarre A, Ueda T, Nakano A, Jurgens G (2003) The Arabidopsis GNOM ARF-GEF mediates endosomal recycling, auxin transport, and auxin-dependent plant growth. Cell **112:** 219-230

Geldner N, Friml J, Stierhof YD, Jurgens G, Palme K (2001) Auxin transport inhibitors block PIN1 cycling and vesicle trafficking. Nature **413:** 425-428

Hayashi K (2012) The interaction and integration of auxin signaling components. Plant Cell Physiol **53:** 965-975

Hayashi K, Neve J, Hirose M, Kuboki A, Shimada Y, Kepinski S, Nozaki H (2012) Rational design of an auxin antagonist of the SCF(TIR1) auxin receptor complex. ACS Chem Biol **7:** 590-598

He W, Brumos J, Li H, Ji Y, Ke M, Gong X, Zeng Q, Li W, Zhang X, An F, Wen X, Li P, Chu J, Sun X, Yan C, Yan N, Xie DY, Raikhel N, Yang Z, Stepanova AN, Alonso JM, Guo H (2011) A small-molecule screen identifies L-kynurenine as a competitive inhibitor of TAA1/TAR activity in ethylene-directed auxin biosynthesis and root growth in Arabidopsis. Plant Cell **23:** 3944-3960

Jasik J, Bokor B, Stuchlik S, Micieta K, Turna J, Schmelzer E (2016) Effects of Auxins on PIN-FORMED2 (PIN2) Dynamics Are Not Mediated by Inhibiting PIN2 Endocytosis. Plant Physiol **172:** 1019-1031

Kasahara H (2016) Current aspects of auxin biosynthesis in plants. Biosci Biotechnol Biochem **80:** 34-42

Kitakura S, Vanneste S, Robert S, Lofke C, Teichmann T, Tanaka H, Friml J (2011) Clathrin mediates endocytosis and polar distribution of PIN auxin transporters in Arabidopsis. Plant Cell **23:** 1920-1931

Korasick DA, Enders TA, Strader LC (2013) Auxin biosynthesis and storage forms. J Exp Bot **64:** 2541-2555

Lee S, Sundaram S, Armitage L, Evans JP, Hawkes T, Kepinski S, Ferro N, Napier RM (2014) Defining binding efficiency and specificity of auxins for SCF(TIR1/AFB)-Aux/IAA co-receptor complex formation. ACS Chem Biol **9:** 673-682

Lewis DR, Muday GK (2009) Measurement of auxin transport in Arabidopsis thaliana. Nat Protoc **4:** 437-451

Leyser O (2018) Auxin Signaling. Plant Physiol **176:** 465-479

Lin D, Nagawa S, Chen J, Cao L, Chen X, Xu T, Li H, Dhonukshe P, Yamamuro C, Friml J, Scheres B, Fu Y, Yang Z (2012) A ROP GTPase-dependent auxin signaling pathway regulates the subcellular distribution of PIN2 in Arabidopsis roots. Curr Biol **22:** 1319-1325

Marhavy P, Bielach A, Abas L, Abuzeineh A, Duclercq J, Tanaka H, Parezova M, Petrasek J, Friml J, Kleine-Vehn J, Benkova E (2011) Cytokinin modulates endocytic trafficking of PIN1 auxin efflux carrier to control plant organogenesis. Dev Cell **21:** 796-804

Muir RM, Fujita T, Hansch C (1967) Structure-activity relationship in the auxin activity of mono-substituted phenylacetic acids. Plant Physiol **42:** 1519-1526

Nagawa S, Xu T, Lin D, Dhonukshe P, Zhang X, Friml J, Scheres B, Fu Y, Yang Z (2012) ROP GTPase-dependent actin microfilaments promote PIN1 polarization by localized inhibition of

clathrin-dependent endocytosis. PLoS Biol **10:** e1001299

Naramoto S, Kleine-Vehn J, Robert S, Fujimoto M, Dainobu T, Paciorek T, Ueda T, Nakano A, Van Montagu MC, Fukuda H, Friml J (2010) ADP-ribosylation factor machinery mediates endocytosis in plant cells. Proc Natl Acad Sci U S A **107:** 21890-21895

Nishimura K, Fukagawa T, Takisawa H, Kakimoto T, Kanemaki M (2009) An auxin-based degron system for the rapid depletion of proteins in nonplant cells. Nat Methods **6:** 917-922

Okushima Y, Fukaki H, Onoda M, Theologis A, Tasaka M (2007) ARF7 and ARF19 regulate lateral root formation via direct activation of LBD/ASL genes in Arabidopsis. Plant Cell **19:** 118-130

Paciorek T, Zazimalova E, Ruthardt N, Petrasek J, Stierhof YD, Kleine-Vehn J, Morris DA, Emans N, Jurgens G, Geldner N, Friml J (2005) Auxin inhibits endocytosis and promotes its own efflux from cells. Nature **435:** 1251-1256

Pan J, Fujioka S, Peng J, Chen J, Li G, Chen R (2009) The E3 ubiquitin ligase SCFTIR1/AFB and membrane sterols play key roles in auxin regulation of endocytosis, recycling, and plasma membrane accumulation of the auxin efflux transporter PIN2 in Arabidopsis thaliana. Plant Cell **21:** 568-580

Prat T, Hajny J, Grunewald W, Vasileva M, Molnar G, Tejos R, Schmid M, Sauer M, Friml J (2018) WRKY23 is a component of the transcriptional network mediating auxin feedback on PIN polarity. PLoS Genet **14:** e1007177

Quareshy M, Uzunova V, Prusinska JM, Napier RM (2017) Assaying Auxin Receptor Activity Using SPR Assays with F-Box Proteins and Aux/IAA Degrons. Methods Mol Biol **1497:** 159-191

Rakusova H, Abbas M, Han H, Song S, Robert HS, Friml J (2016) Termination of Shoot Gravitropic Responses by Auxin Feedback on PIN3 Polarity. Curr Biol **26:** 3026-3032

Rakusova H, Fendrych M, Friml J (2015) Intracellular trafficking and PIN-mediated cell polarity during tropic responses in plants. Curr Opin Plant Biol **23:** 116-123

Ren H, Gray WM (2015) SAUR Proteins as Effectors of Hormonal and Environmental Signals in Plant Growth. Mol Plant **8:** 1153-1164

Rigas S, Ditengou FA, Ljung K, Daras G, Tietz O, Palme K, Hatzopoulos P (2013) Root gravitropism and root hair development constitute coupled developmental responses regulated by auxin homeostasis in the Arabidopsis root apex. New Phytol **197:** 1130-1141

Robert HS, Grones P, Stepanova AN, Robles LM, Lokerse AS, Alonso JM, Weijers D, Friml J (2013) Local auxin sources orient the apical-basal axis in Arabidopsis embryos. Curr Biol **23:** 2506-2512

Robert S, Kleine-Vehn J, Barbez E, Sauer M, Paciorek T, Baster P, Vanneste S, Zhang J, Simon S, Covanova M, Hayashi K, Dhonukshe P, Yang Z, Bednarek SY, Jones AM, Luschnig C, Aniento F, Zazimalova E, Friml J (2010) ABP1 mediates auxin inhibition of clathrin-dependent endocytosis in Arabidopsis. Cell **143:** 111-121

Salanenka Y, Verstraeten I, Lofke C, Tabata K, Naramoto S, Glanc M, Friml J (2018) Gibberellin DELLA signaling targets the retromer complex to redirect protein trafficking to the plasma membrane. Proc Natl Acad Sci U S A **115:** 3716-3721

Sauer M, Paciorek T, Benkova E, Friml J (2006) Immunocytochemical techniques for whole-mount in situ

protein localization in plants. Nat Protoc **1:** 98-103

Spartz AK, Lee SH, Wenger JP, Gonzalez N, Itoh H, Inze D, Peer WA, Murphy AS, Overvoorde PJ, Gray WM (2012) The SAUR19 subfamily of SMALL AUXIN UP RNA genes promote cell expansion. Plant J **70:** 978-990

Sugawara S, Mashiguchi K, Tanaka K, Hishiyama S, Sakai T, Hanada K, Kinoshita-Tsujimura K, Yu H, Dai X, Takebayashi Y, Takeda-Kamiya N, Kakimoto T, Kawaide H, Natsume M, Estelle M, Zhao Y, Hayashi K, Kamiya Y, Kasahara H (2015) Distinct Characteristics of Indole-3-Acetic Acid and Phenylacetic Acid, Two Common Auxins in Plants. Plant Cell Physiol **56:** 1641-1654

Tsuda E, Yang H, Nishimura T, Uehara Y, Sakai T, Furutani M, Koshiba T, Hirose M, Nozaki H, Murphy AS, Hayashi K (2011) Alkoxy-auxins are selective inhibitors of auxin transport mediated by PIN, ABCB, and AUX1 transporters. J Biol Chem **286:** 2354-2364

Tsugafune S, Mashiguchi K, Fukui K, Takebayashi Y, Nishimura T, Sakai T, Shimada Y, Kasahara H, Koshiba T, Hayashi KI (2017) Yucasin DF, a potent and persistent inhibitor of auxin biosynthesis in plants. Sci Rep **7:** 13992

Vieten A, Vanneste S, Wisniewska J, Benkova E, Benjamins R, Beeckman T, Luschnig C, Friml J (2005) Functional redundancy of PIN proteins is accompanied by auxin-dependent cross-regulation of PIN expression. Development **132:** 4521-4531

Winicur ZM, Zhang GF, Staehelin LA (1998) Auxin deprivation induces synchronous Golgi differentiation in suspension-cultured tobacco BY-2 cells. Plant Physiol **117:** 501-513

Wisniewska J, Xu J, Seifertova D, Brewer PB, Ruzicka K, Blilou I, Rouquie D, Benkova E, Scheres B, Friml J (2006) Polar PIN localization directs auxin flow in plants. Science **312:** 883

FIGURE LEGENDS

Figure 1. Evaluation for auxin activity of PISA on SCF$^{TIR1/AFB}$ pathway.

A, The structures of auxins and pinstatic acid (PISA). B, Effects of PISA on auxin-deficient root phenotypes. Arabidopsis plants were cultured for 5 days on vertical agar plate containing chemicals with or without auxin biosynthesis inhibitors, yucasin DF and Kyn. The values in the parenthesis represents the concentration of chemicals (μM). Bar represents 5 mm. C, Effects of alkyloxy-PAA on auxin-responsive *DR5::GUS* expression. 5d-old *DR5::GUS* seedling was incubated with chemicals for 6h. Methoxy (C1) to pentoxy (C5) PAA derivatives including mPISA and PISA was assessed at 50 μM. D, Quantitative analysis of GUS enzyme activity in *DR5::GUS* line treated with IAA and PISA. Values are the means ± S.D. (n=9) E, *DII-VENUS* seedling was incubated with 10 μM yucasin DF for 3h and then washed with medium. The seedling was incubated with PISA and IAA for another 60 min. Bar represents 500 μm. F, Surface Plasmon Resonance analysis of the auxin-induced interaction between TIR1 and IAA7 degron peptide. The sensorgram shows the effect of 50 μM IAA (green) and 50 μM PISA (blue) on TIR1-DII peptide association and dissociation. The bars show the relative response of PISA to IAA (100%).

Figure 2. Effects of PISA on hypocotyl elongation and adventitious root formation.

A, Arabidopsis seedlings cultured for 7 days with PISA. The values in the parenthesis represent the concentration of chemicals (μM). Bar represents 5 mm. B, 13d-old plants grown with PISA. C, Time course of hypocotyl length of seedlings cultured with PISA (closed square:10 μM and closed triangle: 20 μM). Values are the means ± S.D. (n=15-20). D, Hypocotyl lengths of seedlings cultured for 7 days with PISA and auxins. The hypocotyl length (mm) of the mock treated seedlings is indicated. Box-and-whisker plots show a median (centerline), upper/lower quartiles (box limits) and maximum/minimum (whiskers). (n=30-38). Statistical significance assessed by Welch's two sample t-test. Asterisks indicate significant differences (**p<0.05, *p<0.01). E, Etiolated seedlings cultured for 5 days in dark with PISA and auxins. F, Hypocotyl lengths of etiolated seedling cultured for 3 days in dark with PISA and auxins. Statistical significance assessed by Welch's two sample t-test. Asterisks indicate significant differences (n=50-72, **p<0.05, *p<0.01). G, Adventitious root production induced by PISA. Arabidopsis seedlings were cultured for 7 days with PISA and the adventitious root number at shoot and root junction was counted. Asterisks indicate significant differences (n=30, **p<0.05, *p<0.01).

Figure 3. Auxin signaling and transport inhibitors repress PISA-induced hypocotyl phenotypes and PISA promotes basipetal auxin transport in hypocotyl.

A, The hypocotyl length of Arabidopsis wild-type (WT) and *axr1-3* mutant seedlings cultured for 7 days with chemicals. Relative hypocotyl length is shown as the percentage of that in mock-treated plants (100 %). The actual length (mm) of mock-treated hypocotyl are indicated (n=40-48). B,

Seedlings cultured for 7 days with PISA and auxin transport inhibitor, TIBA. C, Hypocotyl length in seedlings cultured with or without TIBA and PISA. Relative hypocotyl length is shown as the percentage of that in mock-treated plants (100 %). The actual length (mm) of mock-treated hypocotyl were indicated as box-and-whisker plots (n=40-45). Statistical significance assessed by Welch's two sample t-test. Asterisks indicate significant differences (**p<0.05, *p<0.01). D, Seedlings of WT, *arf7 arf19* and *slr1/iaa14* mutants cultured for 7 days with or without PISA. The values in the parenthesis represents the concentration of chemicals (μM). Bar represents 5 mm. E, Rootward transport of radiolabeled ^{3}H-IAA in decapitated hypocotyls. NPA, an auxin transport inhibitor, was used as the negative control. (*p<0.01, n=9).

Figure 4. The effects of PISA on root elongation and auxin distribution in root tip.

A, Wild-type seedlings cultured for 7 days with PISA. Bar represents 5 mm. B, Wild-type root cultured with 100 μM PISA . Root was counterstained with propidium iodide. Bar represents 100 μm. C, The primary root length of Arabidopsis wild-type (WT) and auxin mutants (*axr1-3, tir1 afb2, pin3 pin7, pin2/eir1-1* and *aux1-7*) cultured for 7 days on vertical plate containing PISA. Relative root length is shown as the percentage of that in mock-treated plants (100 %). The actual length (mm) of mock-treated root is indicated. Statistical significance was assessed by Welch's two sample t-test between WT and mutants. Asterisks indicate significant differences (n=32-40, **p<0.05, *p<0.01). D, The GFP expression of *DR5::GFP* in roots cultured vertically with PISA for 7 days. Arrows indicate quiescent center (yellow) and lateral root cap (white). Bar represents 100 μm. E, The primary root growth of Arabidopsis WT and auxin mutants during 5 hours on vertical plates containing PISA. The actual length (mm) of mock-treated root is indicated and mock-treated plants shown as 100 %. Asterisks indicate significant differences (n=14-17, *p<0.01). F, The GFP expression of *DR5::GFP* cultured vertically with PISA and TIBA for 20 hours. The values in the parenthesis represents the concentration of chemicals (μM). Bar represents 100 μm.

Figure 5. PISA inhibits root hair formation.

A, Root hairs of *pin2/eir1, 35S::PIN1* and wild-type plants treated with PISA. 5d-old seedlings were cultured for 2 days on vertical agar plates with or without PISA. B, The root hair length and density of *pin2/eir1, 35S::PIN1* and wild-type plants treated with PISA. The length and density of root hairs within the 2-4 mm region from root tip were measured. Values are the means ± S.D. Asterisks indicate significant differences (n=8-11, *p<0.01). The values in the parenthesis represents the concentration of chemicals (μM). C, The root hair formation of wild-type seedlings grown with auxins and auxin transport inhibitors. The values in the parenthesis represents the concentration of chemicals (μM). Bar represents 1 mm.

Figure 6. Effects of PISA on IAA-induced lateral root formation and shootward IAA transport.

A, Effects of PISA on the lateral root formation. Arabidopsis seedlings were cultured for 6 days with

PISA. The number of lateral roots were counted and the density of lateral roots are shown as box-and-whisker plots (n=14-16). (B and C) Effects of PISA on IAA-induced lateral root formation. 5d-old seedlings were cultured for additional 3 days with PISA in the presence of IAA. The density of lateral roots are shown as box-and-whisker plots (n=14-16). Bar represents 5 mm. D, Effects of PISA on IAA-induced *DR5::GUS* expression. 5d-old *DR5::GUS* seedlings were incubated for 12 h in liquid GM medium with or without PISA or auxin transport inhibitors. IAA was added to the GM medium and the seedlings were further incubated for additional 6 h. The IAA-induced GUS activity was visualized by X-Gluc. Bar represents 1 mm. E, Effects of PISA on shootward IAA transport. An agar block containing IAA was applied to *DR5::GUS* root tips (yellow ring) and the seedlings were incubated on vertical plates containing 40 μM PISA for 10 h. Arrows show the IAA-induced GUS activity. Bar represents 1 mm. Statistical significance assessed by Welch's two sample t-test. Asterisks indicate significant differences (*p<0.01). The values in the parenthesis represents the concentration of chemicals (μM).

Figure 7. PISA inhibits auxin distribution and root gravitropism.

A, Effect of PISA on auxin asymmetric distribution. 4-d old *DR5::GFP* seedlings were transferred to 20 μM PISA and control medium for 1h. After 1h seedlings were gravistimulated for 4h and imaged. PISA pretreatment abolished auxin asymmetric distribution and seedlings did not respond to gravity stimuli. B, Quantitative evaluation of A, showing a mean ratio of the signal intensity of the upper/lower half of the root. (*p<0.01). C, Effect of PISA on root gravitropic response. 5-d old wild-type seedlings were placed on vertical GM agar plates containing PISA and then cultured for 3h in the dark. The plates were further incubated for 16h after rotating plates at 135° angle against vertical direction. The arrows indicate the vector of gravity before (1) and after (2) the initiation of gravistimulation. The angles were grouped into 30° classes and plotted as circular histograms.

Figure 8. Effects of PISA on PIN internalization from plasma membrane.

A and B, Effect of PISA on the BFA body formation of PIN2-GFP. 5d-old *proPIN2::PIN2-GFP* seedlings were incubated for 30 min. in liquid GM medium containing PISA and NAA and then BFA was added to the medium. Seedlings were then incubated for additional 60 min. BFA induced PIN2-GFP-marked BFA bodies. The area of BFA body was measured and the area in BFA-treated seedling (n=25-40, *p<0.01) was adjusted to 100 %. The average value of the area was indicated in B. Bar represents 50 μm. C and D, Effect of PISA on the internalization of PIN2-GFP. 5d-old *pPIN2::PIN2-GFP* seedlings were incubated for 12h with PISA. The fluorescence intensity of the apical and lateral sides of cells in the root (n=18-20, *p<0.01) were quantified and the fluorescent signal rate (apical side / lateral side) was indicated in D. The values in the parenthesis represents the concentration of chemicals (μM). Bar represents 50 μm. E, Effects of PISA on a collapse of the primary root meristem. 5d-old root tips of WT and *35S::PID* plants grown vertically on agar plate

847 containing PISA. Bar represents 500 µm. F, Effects of PISA on PIN1 localization in the endodermis of
848 WT and *35S::PID* roots. Immunolocalization of PIN1 after treatment with PISA for 4 h. Bar represents
849 10 µm.
850
851

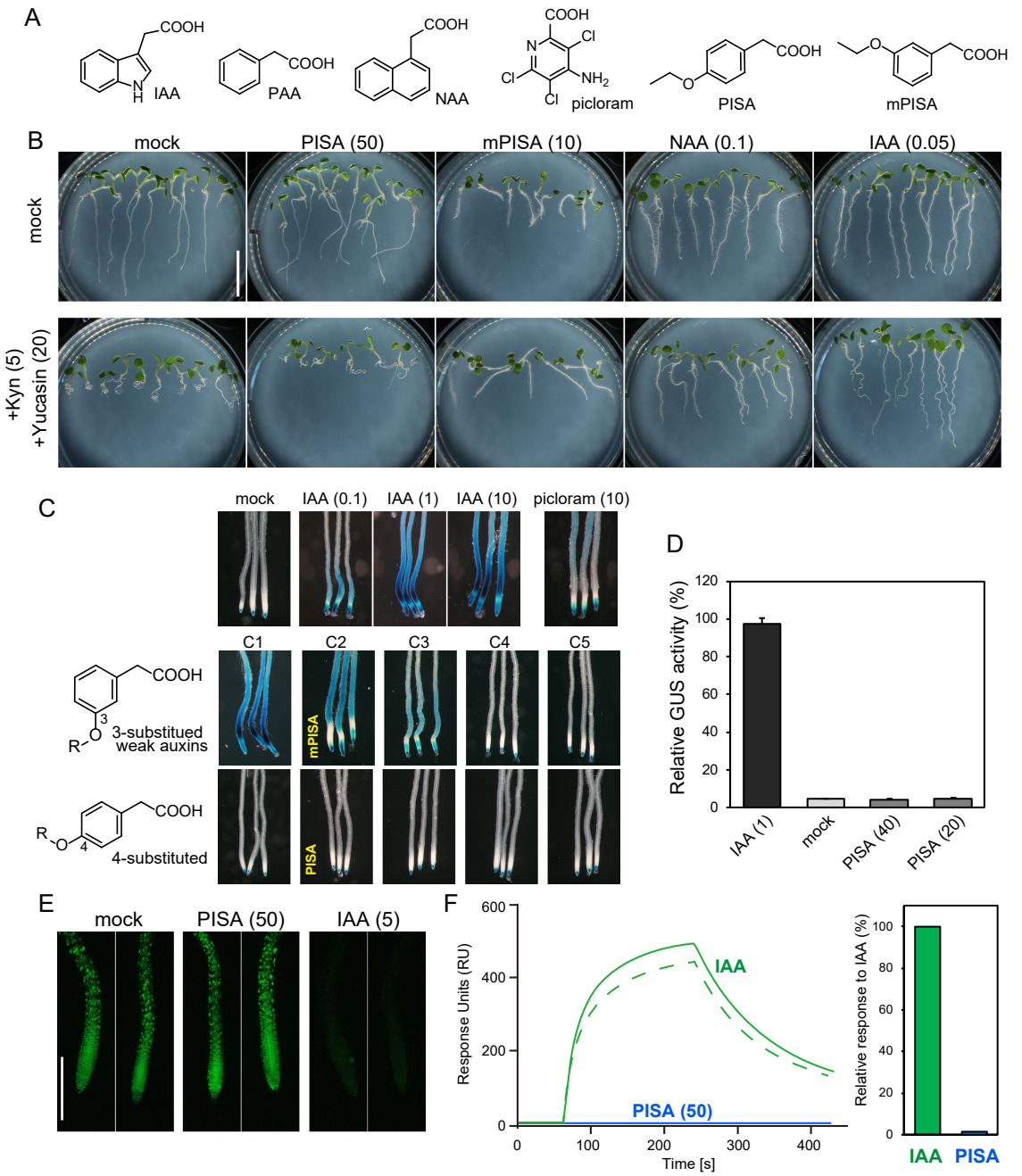

Figure 1. Evaluation for auxin activity of PISA on SCFTIR1/AFB pathway.
A, The structures of auxins and pinstatic acid (PISA). B, Effects of PISA on auxin-deficient root phenotypes. Arabidopsis plants were cultured for 5 days on vertical agar plate containing chemicals with or without auxin biosynthesis inhibitors, yucasin DF and Kyn. The values in the parenthesis represents the concentration of chemicals (μM). Bar represents 5 mm. C, Effects of alkyloxy-PAA on auxin-responsive *DR5::GUS* expression. 5d-old *DR5::GUS* seedling was incubated with chemicals for 6h. Methoxy (C1) to pentoxy (C5) PAA derivatives including mPISA and PISA was assessed at 50 μM. D, Quantitative analysis of GUS enzyme activity in *DR5::GUS* line treated with IAA and PISA. Values are the means ± S.D. (n=9) E, *DII-VENUS* seedling was incubated with 10 μM yucasin DF for 3h and then washed with medium. The seedling was incubated with PISA and IAA for another 60 min. Bar represents 500 μm. F, Surface Plasmon Resonance analysis of the auxin-induced interaction between TIR1 and IAA7 degron peptide. The sensorgram shows the effect of 50 μM IAA (green) and 50 μM PISA (blue) on TIR1-DII peptide association and dissociation. The bars show the relative response of PISA to IAA (100%).

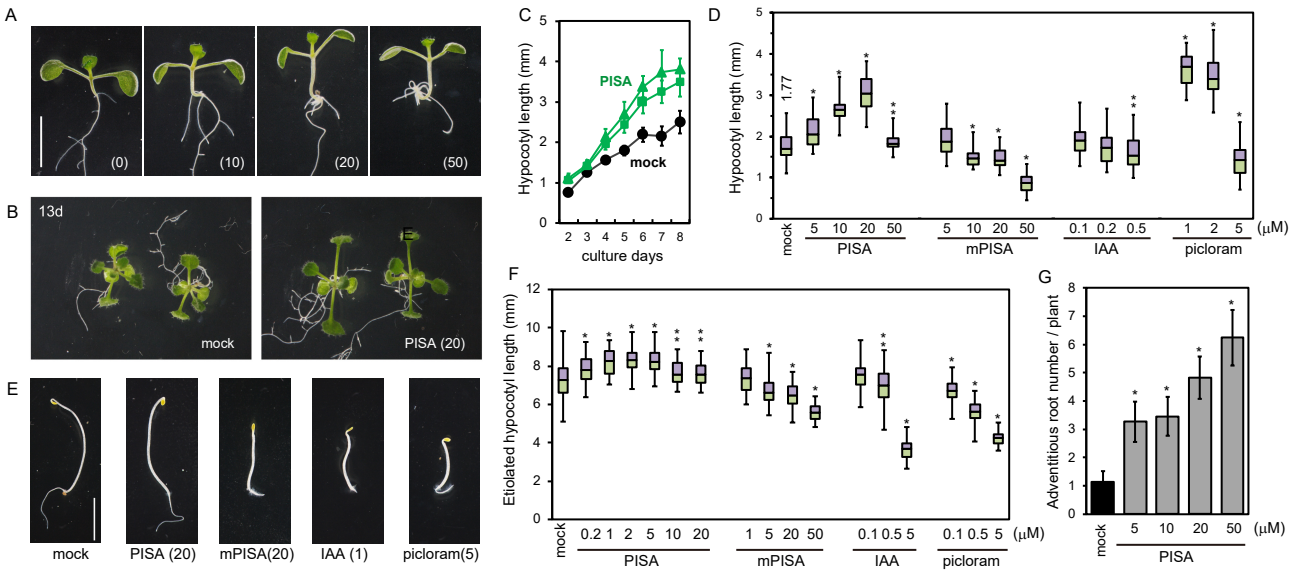

Figure 2. Effects of PISA on hypocotyl elongation and adventitious root formation.
A, Arabidopsis seedlings cultured for 7 days with PISA. The values in the parenthesis represent the concentration of chemicals (μM). Bar represents 5 mm. B, 13d-old plants grown with PISA. C, Time course of hypocotyl length of seedlings cultured with PISA (closed square:10 μM and closed triangle: 20 μM). Values are the means ± S.D. (n=15-20). D, Hypocotyl lengths of seedlings cultured for 7 days with PISA and auxins. The hypocotyl length (mm) of the mock treated seedlings is indicated. Box-and-whisker plots show a median (centerline), upper/lower quartiles (box limits) and maximum/minimum (whiskers). (n=30-38). Statistical significance assessed by Welch's two sample t-test. Asterisks indicate significant differences (**p<0.05, *p<0.01). E, Etiolated seedlings cultured for 5 days in dark with PISA and auxins. F, Hypocotyl lengths of etiolated seedling cultured for 3 days in dark

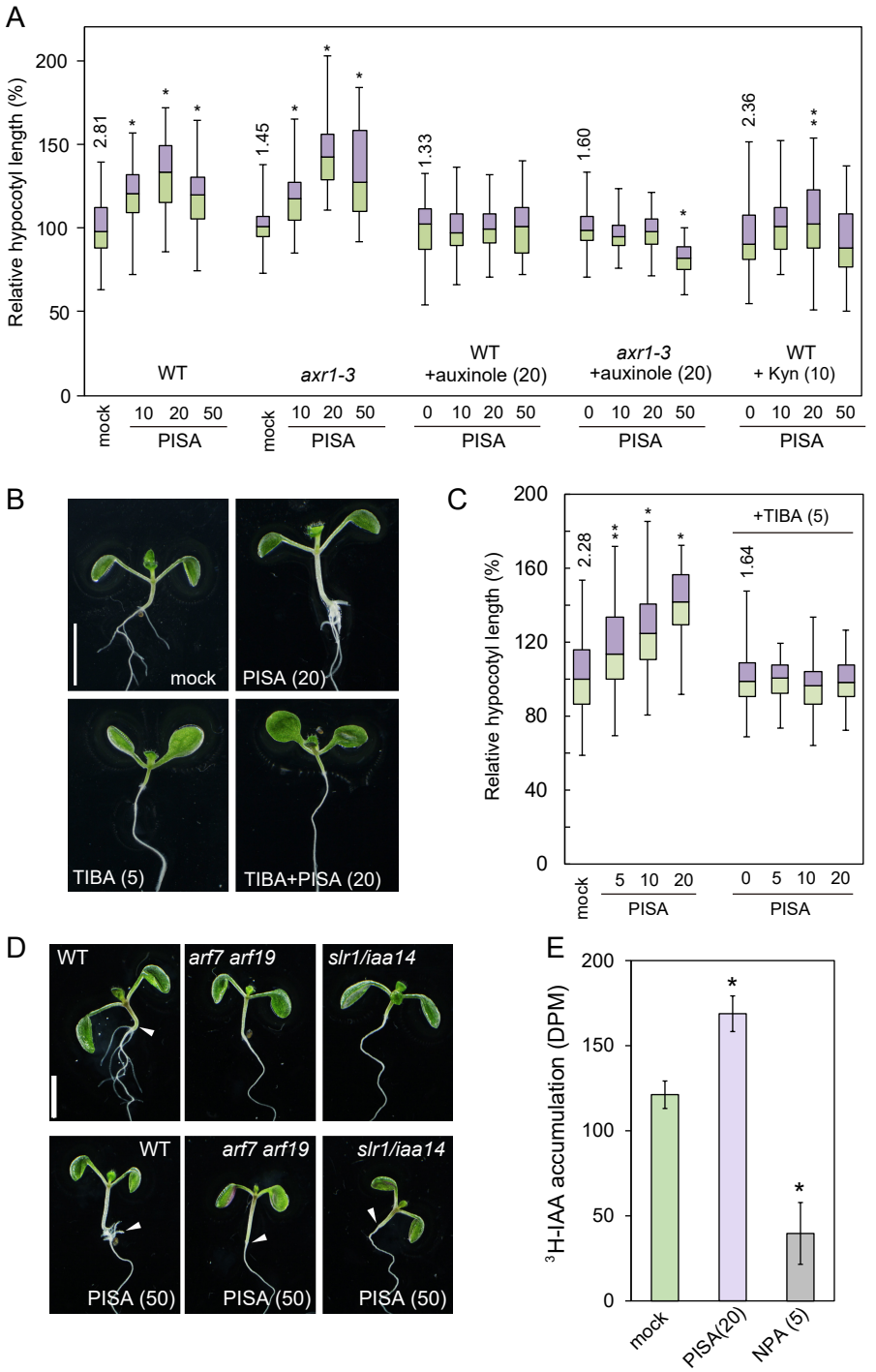

Figure 3. Auxin signaling and transport inhibitors repress PISA-induced hypocotyl phenotypes and PISA promotes basipetal auxin transport in hypocotyl.

A, The hypocotyl length of Arabidopsis wild-type (WT) and *axr1-3* mutant seedlings cultured for 7 days with chemicals. Relative hypocotyl length is shown as the percentage of that in mock-treated plants (100 %). The actual length (mm) of mock-treated hypocotyl are indicated (n=40-48). B, Seedlings cultured for 7 days with PISA and auxin transport inhibitor, TIBA. C, Hypocotyl length in seedlings cultured with or without TIBA and PISA. Relative hypocotyl length is shown as the percentage of that in mock-treated plants (100 %). The actual length (mm) of mock-treated hypocotyl were indicated as box-and-whisker plots (n=40-45). Statistical significance assessed by Welch' s two sample t-test. Asterisks indicate significant differences (**p<0.05, *p<0.01). D, Seedlings of WT, *arf7 arf19* and *slr1/iaa14* mutants cultured for 7 days with or without PISA. The values in the parenthesis represents the concentration of chemicals (μM). Bar represents 5 mm. E, Rootward transport of radiolabeled ^{3}H-IAA in decapitated hypocotyls. NPA, an auxin transport inhibitor, was used as the negative control. (*p<0.01, n=9).

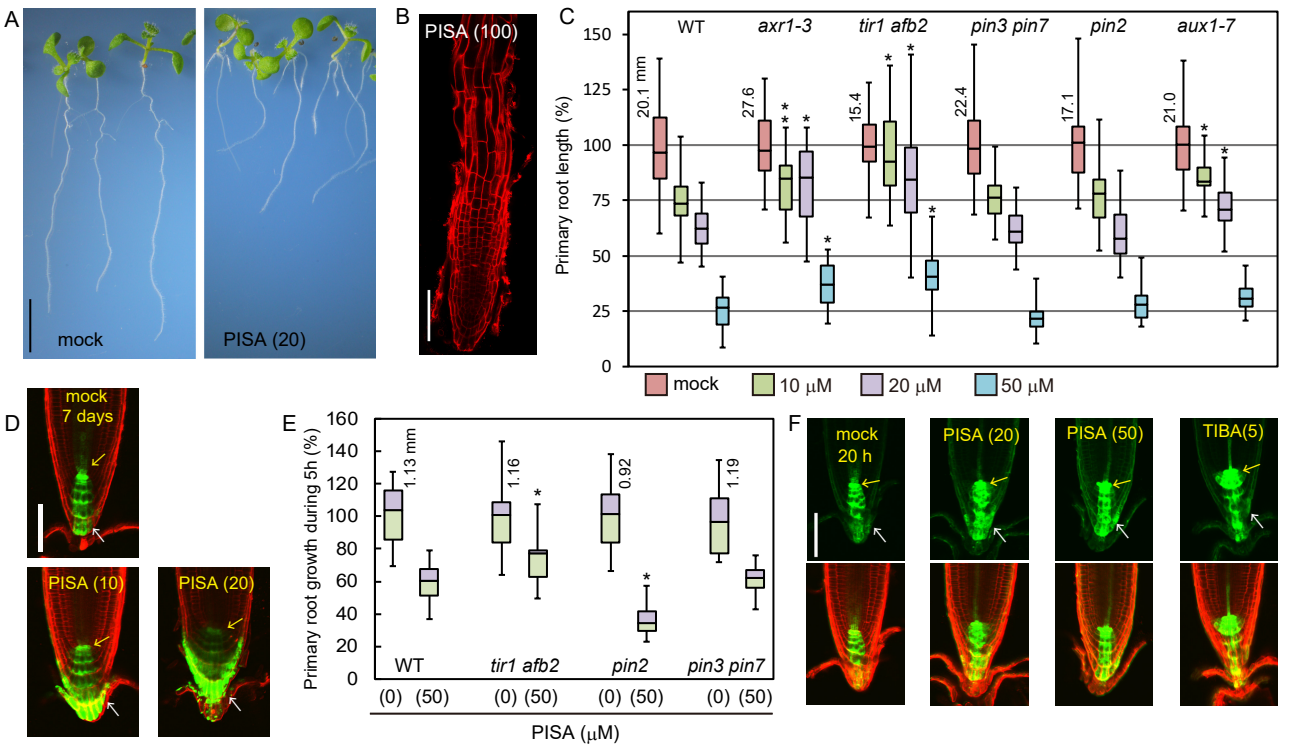

Figure 4. The effects of PISA on root elongation and auxin distribution in root tip.
A, Wild-type seedlings cultured for 7 days with PISA. Bar represents 5 mm. B, Wild-type root cultured with 100 μM PISA . Root was counterstained with propidium iodide. Bar represents 100 μm. C, The primary root length of Arabidopsis wild-type (WT) and auxin mutants (*axr1-3*, *tir1 afb2*, *pin3 pin7*, *pin2/eir1-1* and *aux1-7*) cultured for 7 days on vertical plate containing PISA. Relative root length is shown as the percentage of that in mock-treated plants (100 %). The actual length (mm) of mock-treated root is indicated. Statistical significance was assessed by Welch' s two sample t-test between WT and mutants. Asterisks indicate significant differences (n=32-40, **p<0.05, *p<0.01). D, The GFP expression of *DR5::GFP* in roots cultured vertically with PISA for 7 days. Arrows indicate quiescent center (yellow) and lateral root cap (white). Bar represents 100 μm. E, The primary root growth of Arabidopsis WT and auxin mutants during 5 hours on vertical plates containing PISA. The actual length (mm) of mock-treated root is indicated and mock-treated plants shown as 100 %. Asterisks indicate significant differences (n=14-17, *p<0.01). F, The GFP expression of *DR5::GFP* cultured vertically with PISA and TIBA for 20 hours. The values in the parenthesis represents the concentration of chemicals (μM). Bar represents 100 μm.

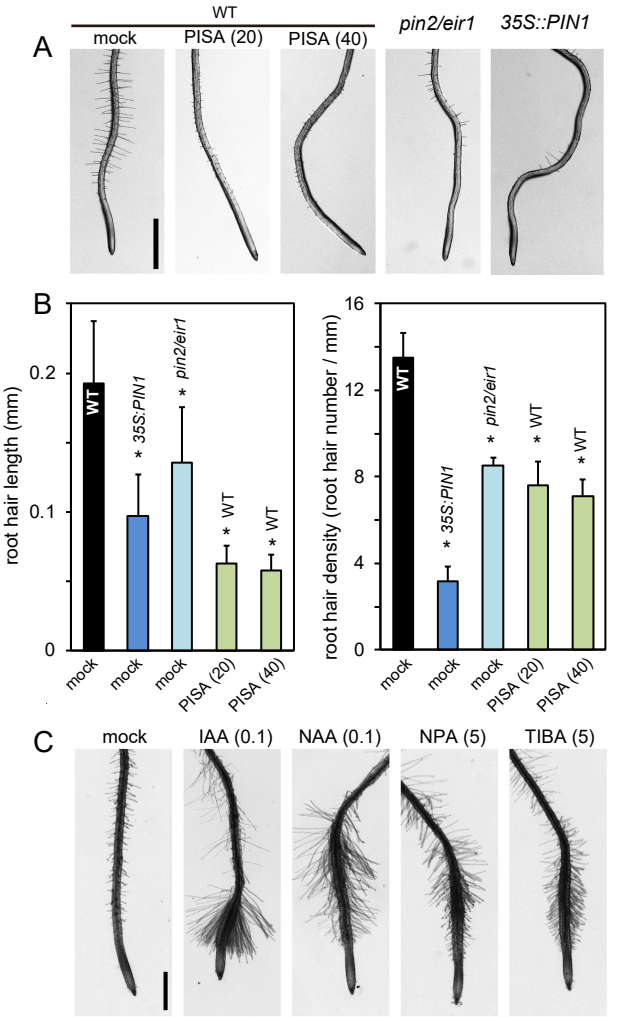

Figure 5. PISA inhibits root hair formation.
A, Root hairs of *pin2/eir1*, *35S::PIN1* and wild-type plants treated with PISA. 5d-old seedlings were cultured for 2 days on vertical agar plates with or without PISA. B, The root hair length and density of *pin2/eir1*, *35S::PIN1* and wild-type plants treated with PISA. The length and density of root hairs within the 2-4 mm region from root tip were measured. Values are the means ± S.D. Asterisks indicate significant differences (n=8-11, *p<0.01). The values in the parenthesis represents the concentration of chemicals (μM). C, The root hair formation of wild-type seedlings grown with auxins and auxin transport inhibitors. The values in the parenthesis represents the concentration of chemicals (μM). Bar represents 1 mm.

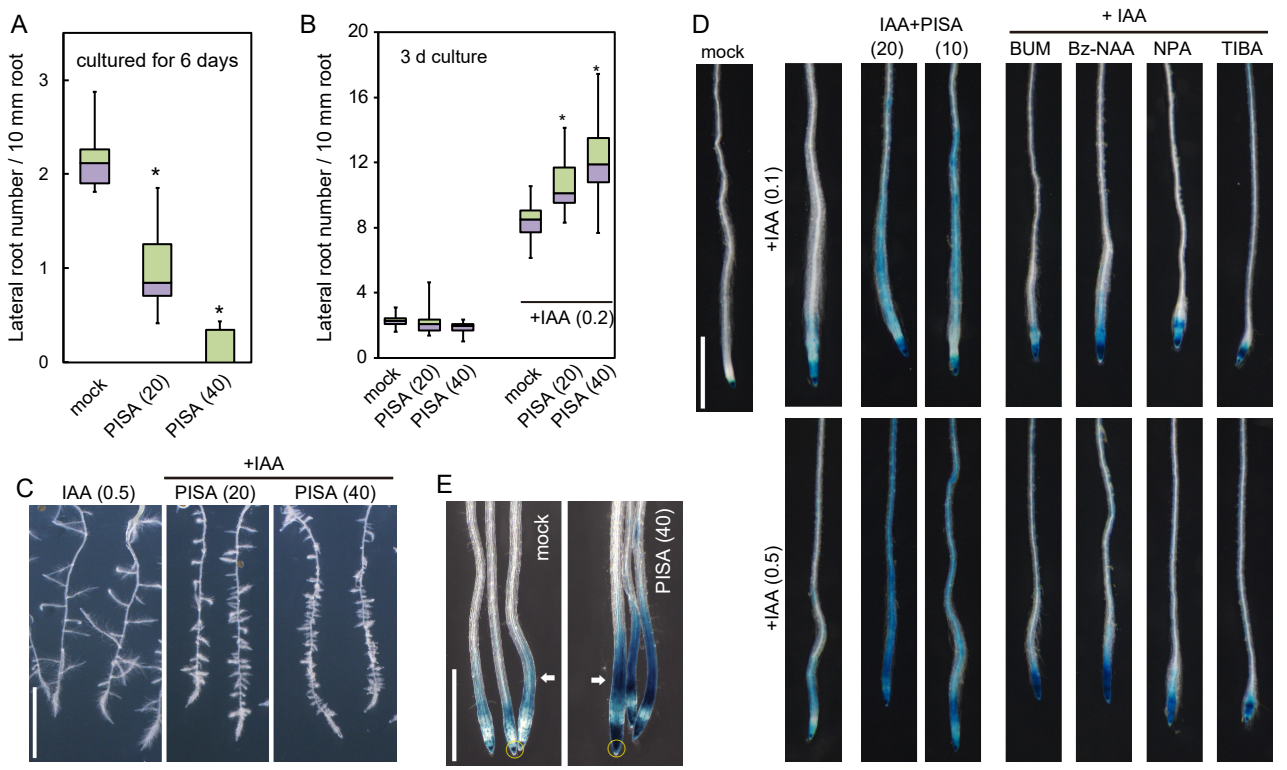

Figure 6. Effects of PISA on IAA-induced lateral root formation and shootward IAA transport.

A, Effects of PISA on the lateral root formation. Arabidopsis seedlings were cultured for 6 days with PISA. The number of lateral roots were counted and the density of lateral roots are shown as box-and-whisker plots (n=14-16). (B and C) Effects of PISA on IAA-induced lateral root formation. 5d-old seedlings were cultured for additional 3 days with PISA in the presence of IAA. The density of lateral roots are shown as box-and-whisker plots (n=14-16). Bar represents 5 mm. D, Effects of PISA on IAA-induced *DR5::GUS* expression. 5d-old *DR5::GUS* seedlings were incubated for 12 h in liquid GM medium with or without PISA or auxin transport inhibitors. IAA was added to the GM medium and the seedlings were further incubated for additional 6 h. The IAA-induced GUS activity was visualized by X-Gluc. Bar represents 1 mm. E, Effects of PISA on shootward IAA transport. An agar block containing IAA was applied to *DR5::GUS* root tips (yellow ring) and the seedlings were incubated on vertical plates containing 40 μM PISA for 10 h. Arrows show the IAA-induced GUS activity. Bar represents 1 mm. Statistical significance assessed by Welch' s two sample t-test. Asterisks indicate significant differences (*p<0.01). The values in the parenthesis represents the concentration of chemicals (μM).

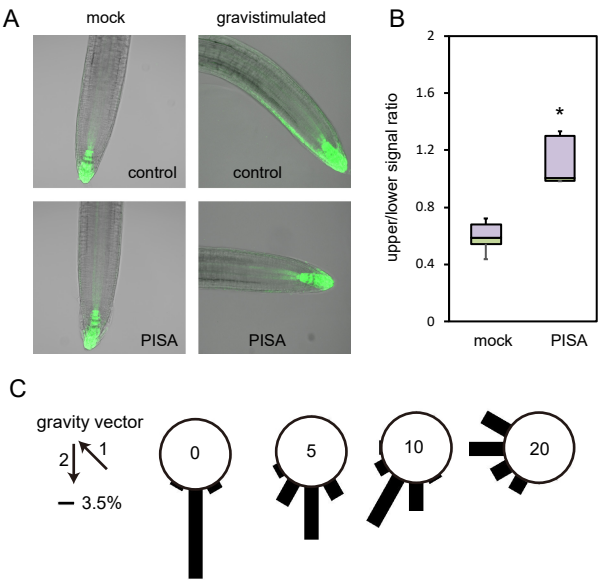

Figure 7. PISA inhibits auxin distribution and root gravitropism.
A, Effect of PISA on auxin asymmetric distribution. 4-d old *DR5::GFP* seedlings were transferred to 20 μM PISA and control medium for 1h. After 1h seedlings were gravistimulated for 4h and imaged. PISA pretreatment abolished auxin asymmetric distribution and seedlings did not respond to gravity stimuli. B, Quantitative evaluation of A, showing a mean ratio of the signal intensity of the upper/lower half of the root. (*p<0.01). C, Effect of PISA on root gravitropic response. 5-d old wild-type seedlings were placed on vertical GM agar plates containing PISA and then cultured for 3h in the dark. The plates were further incubated for 16h after rotating plates at 135° angle against vertical direction. The arrows indicate the vector of gravity before (1) and after (2) the initiation of gravistimulation. The angles were grouped into 30° classes and plotted as circular histograms.

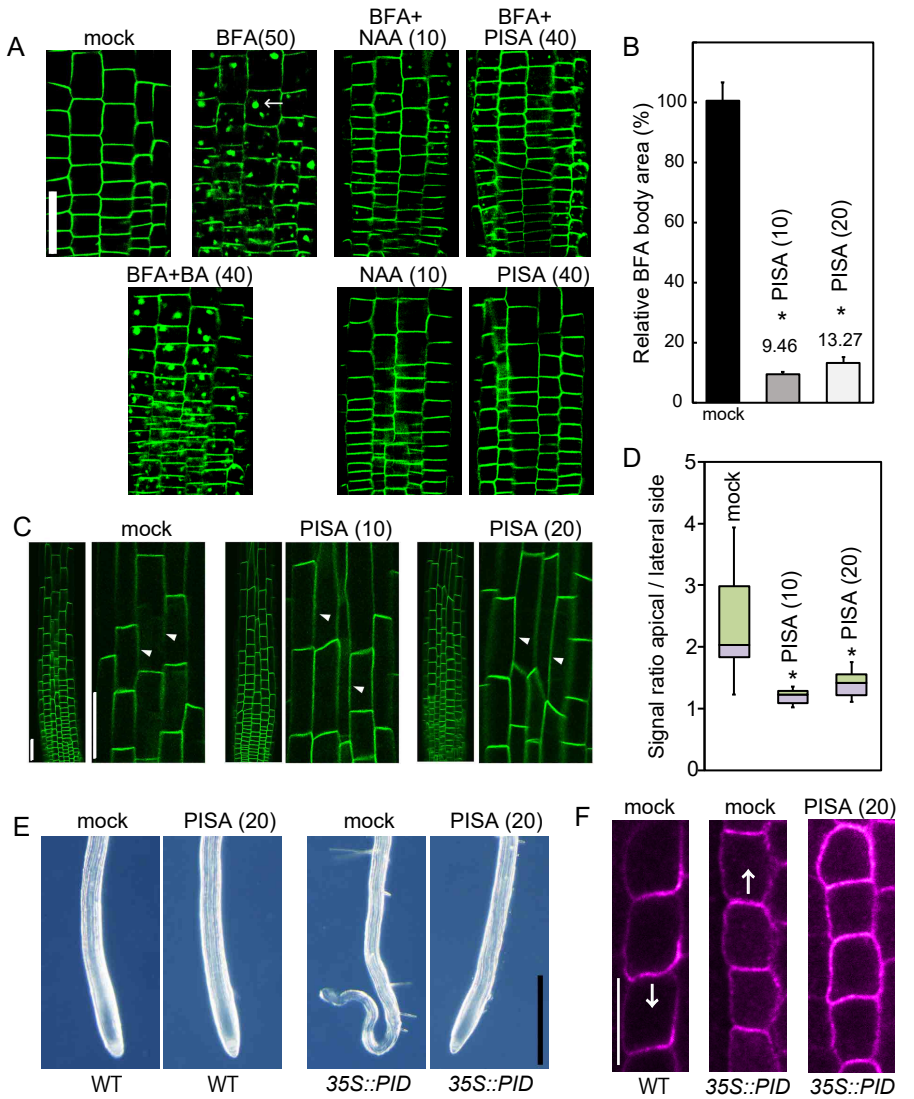

Figure 8. Effects of PISA on PIN internalization from plasma membrane.
A and B, Effect of PISA on the BFA body formation of PIN2-GFP. 5d-old *proPIN2::PIN2-GFP* seedlings were incubated for 30 min. in liquid GM medium containing PISA and NAA and then BFA was added to the medium. Seedlings were then incubated for additional 60 min. BFA induced PIN2-GFP-marked BFA bodies. The area of BFA body was measured and the area in BFA-treated seedling (n=25-40, *p<0.01) was adjusted to 100 %. The average value of the area was indicated in B. Bar represents 50 μm. C and D, Effect of PISA on the internalization of PIN2-GFP. 5d-old *pPIN2::PIN2-GFP* seedlings were incubated for 12h with PISA. The fluorescence intensity of the apical and lateral sides of cells in the root (n=18-20, *p<0.01) were quantified and the fluorescent signal rate (apical side / lateral side) was indicated in D. The values in the parenthesis represents the concentration of chemicals (μM). Bar represents 50 μm. E, Effects of PISA on a collapse of the primary root meristem. 5d-old root tips of WT and *35S::PID* plants grown vertically on agar plate containing PISA. Bar represents 500 μm. F, Effects of PISA on PIN1 localization in the endodermis of WT and *35S::PID* roots. Immunolocalization of PIN1 after treatment with PISA for 4 h. Bar represents 10 μm.

Table 1

Effect of PISA on adventitious root formation at shoot/root junction

	WT (Col)	*arf7 arf19*	*slr1/iaa14*	TIBA (5)	NPA (5)
mock	1.57∓0.65 [a)]	0	0	0	0
PISA (20)	3.21∓0.70	0	0	0	0
PISA (50)	5.07∓1.03	0	0	0	0

a) adventitious root number at shoot/root junction for each 6-d old seedlings

Parsed Citations

Abas L, Benjamins R, Malenica N, Paciorek T, Wisniewska J, Moulinier-Anzola JC, Sieberer T, Friml J, Luschnig C (2006) Intracellular trafficking and proteolysis of the Arabidopsis auxin-efflux facilitator PIN2 are involved in root gravitropism. Nat Cell Biol 8: 249-256
Pubmed: Author and Title
Google Scholar: Author Only Title Only Author and Title

Adamowski M, Friml J (2015) PIN-dependent auxin transport: action, regulation, and evolution. Plant Cell 27: 20-32
Pubmed: Author and Title
Google Scholar: Author Only Title Only Author and Title

Adamowski M, Narasimhan M, Kania U, Glanc M, De Jaeger G, Friml J (2018) A Functional Study of AUXILIN-LIKE1 and 2, Two Putative Clathrin Uncoating Factors in Arabidopsis. Plant Cell 30: 700-716
Pubmed: Author and Title
Google Scholar: Author Only Title Only Author and Title

Baster P, Robert S, Kleine-Vehn J, Vanneste S, Kania U, Grunewald W, De Rybel B, Beeckman T, Friml J (2013) SCF(TIR1/AFB)-auxin signalling regulates PIN vacuolar trafficking and auxin fluxes during root gravitropism. EMBO J 32: 260-274
Pubmed: Author and Title
Google Scholar: Author Only Title Only Author and Title

Benjamins R, Quint A, Weijers D, Hooykaas P, Offringa R (2001) The PINOID protein kinase regulates organ development in Arabidopsis by enhancing polar auxin transport. Development 128: 4057-4067
Pubmed: Author and Title
Google Scholar: Author Only Title Only Author and Title

Brumos J, Robles LM, Yun J, Vu TC, Jackson S, Alonso JM, Stepanova AN (2018) Local Auxin Biosynthesis Is a Key Regulator of Plant Development. Dev Cell 47: 306-318 e305
Pubmed: Author and Title
Google Scholar: Author Only Title Only Author and Title

Brunoud G, Wells DM, Oliva M, Larrieu A, Mirabet V, Burrow AH, Beeckman T, Kepinski S, Traas J, Bennett MJ, Vernoux T (2012) A novel sensor to map auxin response and distribution at high spatio-temporal resolution. Nature 482: 103-106
Pubmed: Author and Title
Google Scholar: Author Only Title Only Author and Title

Buer CS, Muday GK (2004) The transparent testa4 mutation prevents flavonoid synthesis and alters auxin transport and the response of Arabidopsis roots to gravity and light. Plant Cell 16: 1191-1205
Pubmed: Author and Title
Google Scholar: Author Only Title Only Author and Title

Chae K, Isaacs CG, Reeves PH, Maloney GS, Muday GK, Nagpal P, Reed JW (2012) Arabidopsis SMALL AUXIN UP RNA63 promotes hypocotyl and stamen filament elongation. Plant J 71: 684-697
Pubmed: Author and Title
Google Scholar: Author Only Title Only Author and Title

Chen Q, Dai X, De-Paoli H, Cheng Y, Takebayashi Y, Kasahara H, Kamiya Y, Zhao Y (2014) Auxin overproduction in shoots cannot rescue auxin deficiencies in Arabidopsis roots. Plant Cell Physiol 55: 1072-1079
Pubmed: Author and Title
Google Scholar: Author Only Title Only Author and Title

Ding Z, Galvan-Ampudia CS, Demarsy E, Langowski L, Kleine-Vehn J, Fan Y, Morita MT, Tasaka M, Fankhauser C, Offringa R, Friml J (2011) Light-mediated polarization of the PIN3 auxin transporter for the phototropic response in Arabidopsis. Nat Cell Biol 13: 447-452
Pubmed: Author and Title
Google Scholar: Author Only Title Only Author and Title

Du Y, Tejos R, Beck M, Himschoot E, Li H, Robatzek S, Vanneste S, Friml J (2013) Salicylic acid interferes with clathrin-mediated endocytic protein trafficking. Proc Natl Acad Sci U S A 110: 7946-7951
Pubmed: Author and Title
Google Scholar: Author Only Title Only Author and Title

Fendrych M, Leung J, Friml J (2016) TIR1/AFB-Aux/IAA auxin perception mediates rapid cell wall acidification and growth of Arabidopsis hypocotyls. Elife 5
Pubmed: Author and Title
Google Scholar: Author Only Title Only Author and Title

Friml J, Yang X, Michniewicz M, Weijers D, Quint A, Tietz O, Benjamins R, Ouwerkerk PB, Ljung K, Sandberg G, Hooykaas PJ, Palme K, Offringa R (2004) A PINOID-dependent binary switch in apical-basal PIN polar targeting directs auxin efflux. Science 306: 862-865
Pubmed: Author and Title
Google Scholar: Author Only Title Only Author and Title

Fukui K, Hayashi KI (2018) Manipulation and Sensing of auxin metabolism, transport and signaling. Plant Cell Physiol
Pubmed: Author and Title
Google Scholar: Author Only Title Only Author and Title

Furutani M, Nakano Y, Tasaka M (2014) MAB4-induced auxin sink generates local auxin gradients in Arabidopsis organ formation. Proc Natl Acad Sci U S A 111: 1198-1203
Pubmed: Author and Title
Google Scholar: Author Only Title Only Author and Title

Ganguly A, Lee SH, Cho M, Lee OR, Yoo H, Cho HT (2010) Differential auxin-transporting activities of PIN-FORMED proteins in Arabidopsis root hair cells. Plant Physiol 153: 1046-1061
Pubmed: Author and Title
Google Scholar: Author Only Title Only Author and Title

Geldner N, Anders N, Wolters H, Keicher J, Kornberger W, Muller P, Delbarre A, Ueda T, Nakano A, Jurgens G (2003) The Arabidopsis GNOM ARF-GEF mediates endosomal recycling, auxin transport, and auxin-dependent plant growth. Cell 112: 219-230
Pubmed: Author and Title
Google Scholar: Author Only Title Only Author and Title

Geldner N, Friml J, Stierhof YD, Jurgens G, Palme K (2001) Auxin transport inhibitors block PIN1 cycling and vesicle trafficking. Nature 413: 425-428
Pubmed: Author and Title
Google Scholar: Author Only Title Only Author and Title

Hayashi K (2012) The interaction and integration of auxin signaling components. Plant Cell Physiol 53: 965-975
Pubmed: Author and Title
Google Scholar: Author Only Title Only Author and Title

Hayashi K, Neve J, Hirose M, Kuboki A, Shimada Y, Kepinski S, Nozaki H (2012) Rational design of an auxin antagonist of the SCF(TIR1) auxin receptor complex. ACS Chem Biol 7: 590-598
Pubmed: Author and Title
Google Scholar: Author Only Title Only Author and Title

He W, Brumos J, Li H, Ji Y, Ke M, Gong X, Zeng Q, Li W, Zhang X, An F, Wen X, Li P, Chu J, Sun X, Yan C, Yan N, Xie DY, Raikhel N, Yang Z, Stepanova AN, Alonso JM, Guo H (2011) A small-molecule screen identifies L-kynurenine as a competitive inhibitor of TAA1/TAR activity in ethylene-directed auxin biosynthesis and root growth in Arabidopsis. Plant Cell 23: 3944-3960
Pubmed: Author and Title
Google Scholar: Author Only Title Only Author and Title

Jasik J, Bokor B, Stuchlik S, Micieta K, Turna J, Schmelzer E (2016) Effects of Auxins on PIN-FORMED2 (PIN2) Dynamics Are Not Mediated by Inhibiting PIN2 Endocytosis. Plant Physiol 172: 1019-1031
Pubmed: Author and Title
Google Scholar: Author Only Title Only Author and Title

Kasahara H (2016) Current aspects of auxin biosynthesis in plants. Biosci Biotechnol Biochem 80: 34-42
Pubmed: Author and Title
Google Scholar: Author Only Title Only Author and Title

Kitakura S, Vanneste S, Robert S, Lofke C, Teichmann T, Tanaka H, Friml J (2011) Clathrin mediates endocytosis and polar distribution of PIN auxin transporters in Arabidopsis. Plant Cell 23: 1920-1931
Pubmed: Author and Title
Google Scholar: Author Only Title Only Author and Title

Korasick DA, Enders TA, Strader LC (2013) Auxin biosynthesis and storage forms. J Exp Bot 64: 2541-2555
Pubmed: Author and Title
Google Scholar: Author Only Title Only Author and Title

Lee S, Sundaram S, Armitage L, Evans JP, Hawkes T, Kepinski S, Ferro N, Napier RM (2014) Defining binding efficiency and specificity of auxins for SCF(TIR1/AFB)-Aux/IAA co-receptor complex formation. ACS Chem Biol 9: 673-682
Pubmed: Author and Title
Google Scholar: Author Only Title Only Author and Title

Lewis DR, Muday GK (2009) Measurement of auxin transport in Arabidopsis thaliana. Nat Protoc 4: 437-451
Pubmed: Author and Title
Google Scholar: Author Only Title Only Author and Title

Leyser O (2018) Auxin Signaling. Plant Physiol 176: 465-479
Pubmed: Author and Title
Google Scholar: Author Only Title Only Author and Title

Lin D, Nagawa S, Chen J, Cao L, Chen X, Xu T, Li H, Dhonukshe P, Yamamuro C, Friml J, Scheres B, Fu Y, Yang Z (2012) A ROP GTPase-dependent auxin signaling pathway regulates the subcellular distribution of PIN2 in Arabidopsis roots. Curr Biol 22: 1319-1325
Pubmed: Author and Title
Google Scholar: Author Only Title Only Author and Title

Marhavy P, Bielach A, Abas L, Abuzeineh A, Duclercq J, Tanaka H, Parezova M, Petrasek J, Friml J, Kleine-Vehn J, Benkova E (2011) Cytokinin modulates endocytic trafficking of PIN1 auxin efflux carrier to control plant organogenesis. Dev Cell 21: 796-804
Pubmed: Author and Title

Google Scholar: Author Only Title Only Author and Title

Muir RM, Fujita T, Hansch C (1967) Structure-activity relationship in the auxin activity of mono-substituted phenylacetic acids. Plant Physiol 42: 1519-1526
Pubmed: Author and Title
Google Scholar: Author Only Title Only Author and Title

Nagawa S, Xu T, Lin D, Dhonukshe P, Zhang X, Friml J, Scheres B, Fu Y, Yang Z (2012) ROP GTPase-dependent actin microfilaments promote PIN1 polarization by localized inhibition of clathrin-dependent endocytosis. PLoS Biol 10: e1001299
Pubmed: Author and Title
Google Scholar: Author Only Title Only Author and Title

Naramoto S, Kleine-Vehn J, Robert S, Fujimoto M, Dainobu T, Paciorek T, Ueda T, Nakano A, Van Montagu MC, Fukuda H, Friml J (2010) ADP-ribosylation factor machinery mediates endocytosis in plant cells. Proc Natl Acad Sci U S A 107: 21890-21895
Pubmed: Author and Title
Google Scholar: Author Only Title Only Author and Title

Nishimura K, Fukagawa T, Takisawa H, Kakimoto T, Kanemaki M (2009) An auxin-based degron system for the rapid depletion of proteins in nonplant cells. Nat Methods 6: 917-922
Pubmed: Author and Title
Google Scholar: Author Only Title Only Author and Title

Okushima Y, Fukaki H, Onoda M, Theologis A, Tasaka M (2007) ARF7 and ARF19 regulate lateral root formation via direct activation of LBD/ASL genes in Arabidopsis. Plant Cell 19: 118-130
Pubmed: Author and Title
Google Scholar: Author Only Title Only Author and Title

Paciorek T, Zazimalova E, Ruthardt N, Petrasek J, Stierhof YD, Kleine-Vehn J, Morris DA, Emans N, Jurgens G, Geldner N, Friml J (2005) Auxin inhibits endocytosis and promotes its own efflux from cells. Nature 435: 1251-1256
Pubmed: Author and Title
Google Scholar: Author Only Title Only Author and Title

Pan J, Fujioka S, Peng J, Chen J, Li G, Chen R (2009) The E3 ubiquitin ligase SCFTIR1/AFB and membrane sterols play key roles in auxin regulation of endocytosis, recycling, and plasma membrane accumulation of the auxin efflux transporter PIN2 in Arabidopsis thaliana. Plant Cell 21: 568-580
Pubmed: Author and Title
Google Scholar: Author Only Title Only Author and Title

Prat T, Hajny J, Grunewald W, Vasileva M, Molnar G, Tejos R, Schmid M, Sauer M, Friml J (2018) WRKY23 is a component of the transcriptional network mediating auxin feedback on PIN polarity. PLoS Genet 14: e1007177
Pubmed: Author and Title
Google Scholar: Author Only Title Only Author and Title

Quareshy M, Uzunova V, Prusinska JM, Napier RM (2017) Assaying Auxin Receptor Activity Using SPR Assays with F-Box Proteins and Aux/IAA Degrons. Methods Mol Biol 1497: 159-191
Pubmed: Author and Title
Google Scholar: Author Only Title Only Author and Title

Rakusova H, Abbas M, Han H, Song S, Robert HS, Friml J (2016) Termination of Shoot Gravitropic Responses by Auxin Feedback on PIN3 Polarity. Curr Biol 26: 3026-3032
Pubmed: Author and Title
Google Scholar: Author Only Title Only Author and Title

Rakusova H, Fendrych M, Friml J (2015) Intracellular trafficking and PIN-mediated cell polarity during tropic responses in plants. Curr Opin Plant Biol 23: 116-123
Pubmed: Author and Title
Google Scholar: Author Only Title Only Author and Title

Ren H, Gray WM (2015) SAUR Proteins as Effectors of Hormonal and Environmental Signals in Plant Growth. Mol Plant 8: 1153-1164
Pubmed: Author and Title
Google Scholar: Author Only Title Only Author and Title

Rigas S, Ditengou FA, Ljung K, Daras G, Tietz O, Palme K, Hatzopoulos P (2013) Root gravitropism and root hair development constitute coupled developmental responses regulated by auxin homeostasis in the Arabidopsis root apex. New Phytol 197: 1130-1141
Pubmed: Author and Title
Google Scholar: Author Only Title Only Author and Title

Robert HS, Grones P, Stepanova AN, Robles LM, Lokerse AS, Alonso JM, Weijers D, Friml J (2013) Local auxin sources orient the apical-basal axis in Arabidopsis embryos. Curr Biol 23: 2506-2512
Pubmed: Author and Title
Google Scholar: Author Only Title Only Author and Title

Robert S, Kleine-Vehn J, Barbez E, Sauer M, Paciorek T, Baster P, Vanneste S, Zhang J, Simon S, Covanova M, Hayashi K, Dhonukshe P, Yang Z, Bednarek SY, Jones AM, Luschnig C, Aniento F, Zazimalova E, Friml J (2010) ABP1 mediates auxin inhibition of clathrin-dependent endocytosis in Arabidopsis. Cell 143: 111-121

Pubmed: Author and Title
Google Scholar: Author Only Title Only Author and Title

Salanenka Y, Verstraeten I, Lofke C, Tabata K, Naramoto S, Glanc M, Friml J (2018) Gibberellin DELLA signaling targets the retromer complex to redirect protein trafficking to the plasma membrane. Proc Natl Acad Sci U S A 115: 3716-3721
Pubmed: Author and Title
Google Scholar: Author Only Title Only Author and Title

Sauer M, Paciorek T, Benkova E, Friml J (2006) Immunocytochemical techniques for whole-mount in situ protein localization in plants. Nat Protoc 1: 98-103
Pubmed: Author and Title
Google Scholar: Author Only Title Only Author and Title

Spartz AK, Lee SH, Wenger JP, Gonzalez N, Itoh H, Inze D, Peer WA, Murphy AS, Overvoorde PJ, Gray WM (2012) The SAUR19 subfamily of SMALL AUXIN UP RNA genes promote cell expansion. Plant J 70: 978-990
Pubmed: Author and Title
Google Scholar: Author Only Title Only Author and Title

Sugawara S, Mashiguchi K, Tanaka K, Hishiyama S, Sakai T, Hanada K, Kinoshita-Tsujimura K, Yu H, Dai X, Takebayashi Y, Takeda-Kamiya N, Kakimoto T, Kawaide H, Natsume M, Estelle M, Zhao Y, Hayashi K, Kamiya Y, Kasahara H (2015) Distinct Characteristics of Indole-3-Acetic Acid and Phenylacetic Acid, Two Common Auxins in Plants. Plant Cell Physiol 56: 1641-1654
Pubmed: Author and Title
Google Scholar: Author Only Title Only Author and Title

Tsuda E, Yang H, Nishimura T, Uehara Y, Sakai T, Furutani M, Koshiba T, Hirose M, Nozaki H, Murphy AS, Hayashi K (2011) Alkoxy-auxins are selective inhibitors of auxin transport mediated by PIN, ABCB, and AUX1 transporters. J Biol Chem 286: 2354-2364
Pubmed: Author and Title
Google Scholar: Author Only Title Only Author and Title

Tsugafune S, Mashiguchi K, Fukui K, Takebayashi Y, Nishimura T, Sakai T, Shimada Y, Kasahara H, Koshiba T, Hayashi KI (2017) Yucasin DF, a potent and persistent inhibitor of auxin biosynthesis in plants. Sci Rep 7: 13992
Pubmed: Author and Title
Google Scholar: Author Only Title Only Author and Title

Vieten A, Vanneste S, Wisniewska J, Benkova E, Benjamins R, Beeckman T, Luschnig C, Friml J (2005) Functional redundancy of PIN proteins is accompanied by auxin-dependent cross-regulation of PIN expression. Development 132: 4521-4531
Pubmed: Author and Title
Google Scholar: Author Only Title Only Author and Title

Winicur ZM, Zhang GF, Staehelin LA (1998) Auxin deprivation induces synchronous Golgi differentiation in suspension-cultured tobacco BY-2 cells. Plant Physiol 117: 501-513
Pubmed: Author and Title
Google Scholar: Author Only Title Only Author and Title

Wisniewska J, Xu J, Seifertova D, Brewer PB, Ruzicka K, Blilou I, Rouquie D, Benkova E, Scheres B, Friml J (2006) Polar PIN localization directs auxin flow in plants. Science 312: 883
Pubmed: Author and Title
Google Scholar: Author Only Title Only Author and Title

Pinstatic acid promotes auxin transport by inhibiting PIN internalization

Akihiro Oochi,[a] Jakub Hajny,[b,h] Kosuke Fukui,[a] Yukio Nakao,[a] Michelle Gallei, [b] Mussa Quareshy,[c] Koji Takahashi,[de] Toshinori Kinoshita,[de] Sigurd Ramans Harborough,[f] Stefan Kepinski,[f] Hiroyuki Kasahara,[g] Richard Napier,[c] Jiri Friml,[b] Ken-ichiro Hayashi[a1]

[a]Department of Biochemistry, Okayama University of Science, Okayama 700-0005, Japan.
[b]Institute of Science and Technology Austria, Klosterneuburg, Austria.
[c]School of Life Sciences, University of Warwick, Coventry, CV4 7AL, United Kingdom
[d]Graduate School of Science, Nagoya University, Chikusa, Nagoya, 464-8602 Japan.
[e]Institute of Transformative Bio-Molecules (WPI-ITbM), Nagoya University, Chikusa, Nagoya, 464-8601, Japan.
[f]Centre for Plant Sciences, Faculty of Biological Sciences, University of Leeds, Leeds LS2 9JT, UK.
[g]Institute of Global Innovation Research, Tokyo University of Agriculture and Technology, Fuchu-shi, Tokyo 183-8509, Japan
[h]Laboratory of Growth Regulators, The Czech Academy of Sciences, Institute of Experimental Botany & Palacký University, Šlechtitelů 27, CZ-78371 Olomouc, Czech Republic

Supplemental Figures

Supplemental Methods

References in Supplemental Methods

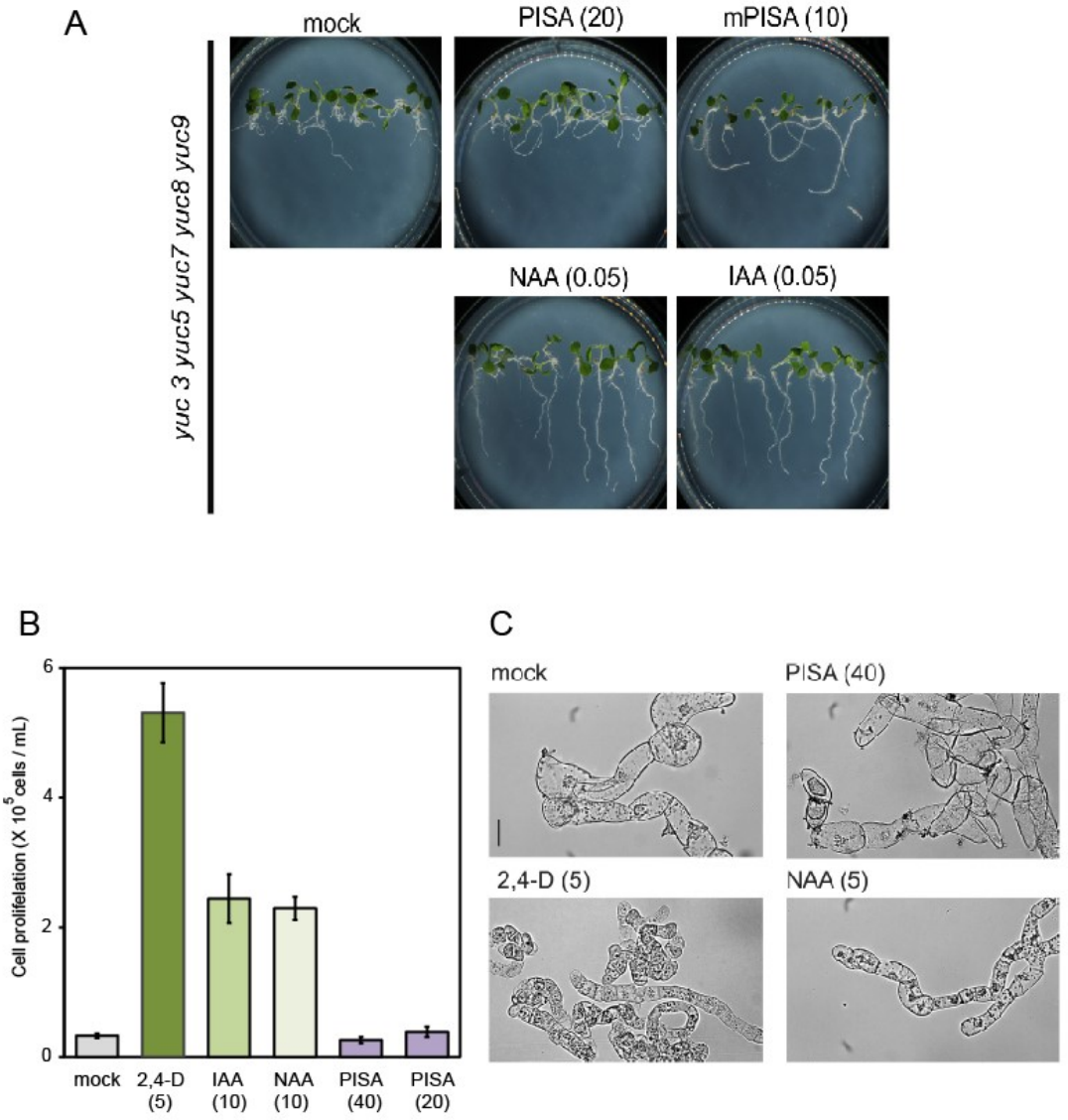

Figure S1. Auxin activity in an auxin-deficient Arabidopsis mutant and BY2 tobacco cell culture.
A, Effect of PISA on auxin-deficient phenotype in *yuc 3 5 7 8 9* (*yucQ*) mutant. Arabidopsis *yucQ* mutant was cultured for 5 days on vertical agar plates containing chemicals. IAA and NAA at 50 nM restored auxin-deficient root phenotypes. mPISA restored the defects in primary root growth, but failed to rescue the agravitropic root. PISA slightly recovered primary root growth defect. The values in the parentheses represent the concentration of chemicals (μM). Bar represents 5 mm. B, Auxin-starved tobacco BY-2 suspension cells cultured without 2,4-D for 24 h were incubated with 2,4-D, NAA and PISA for 4 days. The cell number was counted by hemocytometer. The photographs in (C) are of the same magnification. Bar represents 50 μm.

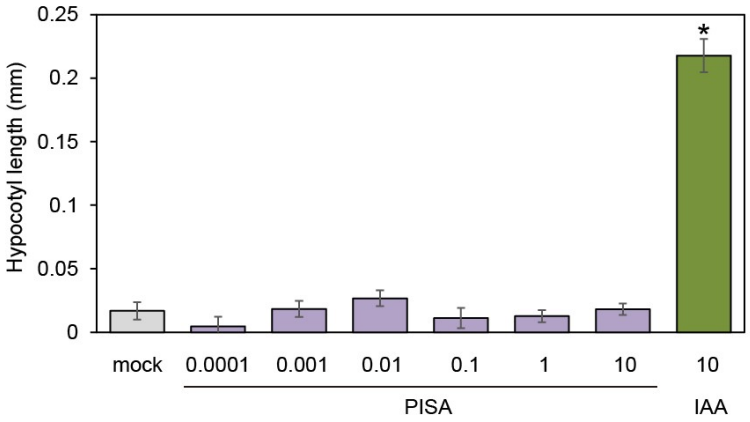

Figure S2. Effects of PISA on rapid cell expansion in hypocotyl.

The hypocotyl sections from 3-d-old etiolated seedlings were treated with PISA or IAA at the indicated concentrations (μM) and the subsequent elongation of the hypocotyl sections for 30 min was measured. Values are the means ±S.E (n=15). Statistical significance assessed by Student's t-test (*$p<0.01$). Experiments were repeated at least three times.

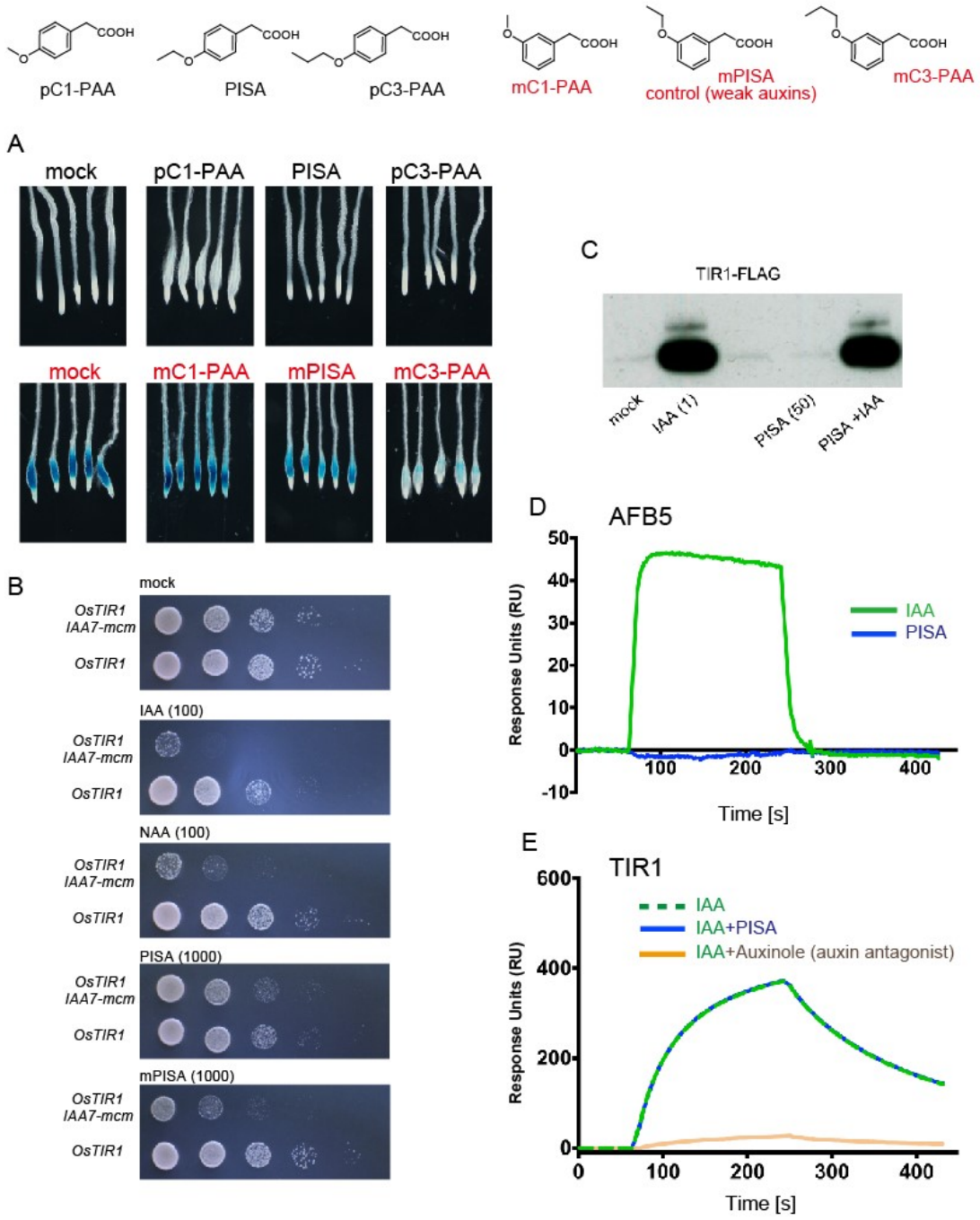

Figure S3. Effects of PISA on SCF^{TIR1} signaling.

A, Effects of PISA on auxin-responsive *BA3::GUS* expression (Oono et al., 1998). 5d-old *BA3::GUS* seedlings were incubated in 1/2 MS liquid medium with the chemicals at 50 μM for 10 h. 4-Alkyloxy PAA, 4-methoxy PAA (pC1-PAA), PISA and 4-propoxy PAA (pC3-PAA) did not induced *BA3::GUS* expression. 3-alkyloxy PAA (meta substituted alkyloxy PAA), 3-methoxy PAA (mC3-PAA), mPISA and 3-propoxy PAA (mC3-PAA) induced *BA3::GUS* expression. B, Effects of PISA on the growth of the yeast expressing OsTIR1 and mcm4-IAA17(aid) fusion proteins (Nishimura et al., 2009). Yeast cells expressing the OsTIR1 from the constitutive ADH1 promoter (control) or both OsTIR1 and mcm4-IAA17 were spotted in serial dilution on a YPD plate with or without chemicals. The values in the parentheses represent the

concentration of chemicals (μM). PISA did not affect the growth of yeast expressing both OsTIR1 and mcm4-IAA17. mPISA, IAA and NAA selectively blocked the growth of yeast cell expressing both OsTIR1 and mcm4-IAA17 by promoting the degradation of mcm4-IAA7 via ubiquitin-proteasome pathway. The values in the parentheses represent the concentration of chemicals (μM). C, Pull-down assay between FLAG-tagged TIR1 and IAA7 (Aux/IAA domain II degron peptide). IAA at 1 μM induced the interaction between TIR1 and IAA7. PISA did not induce the interaction between TIR1 and IAA7. To assess potential anti-auxin activity of PISA, 50 μM PISA was added to lysates 15 minutes prior to the addition of 1 μM IAA and the start of the assay. PISA did not inhibit IAA-induced the interaction between TIR1 and IAA7. D, Surface Plasmon Resonance analysis of the auxin-induced the interaction between AFB5 and IAA7 DII peptide. 50 μM IAA (green) induced the interaction. PISA (blue) did not affect the complex formation. E, The sensorgram shows the effect of 50 μM PISA (blue) in the presence of 5 μM IAA on TIR1-IAA7 DII peptide association and dissociation. Auxinole, auxin antagonist blocked the interaction between TIR1 and IAA7 degron peptide. PISA did not affect the interaction.

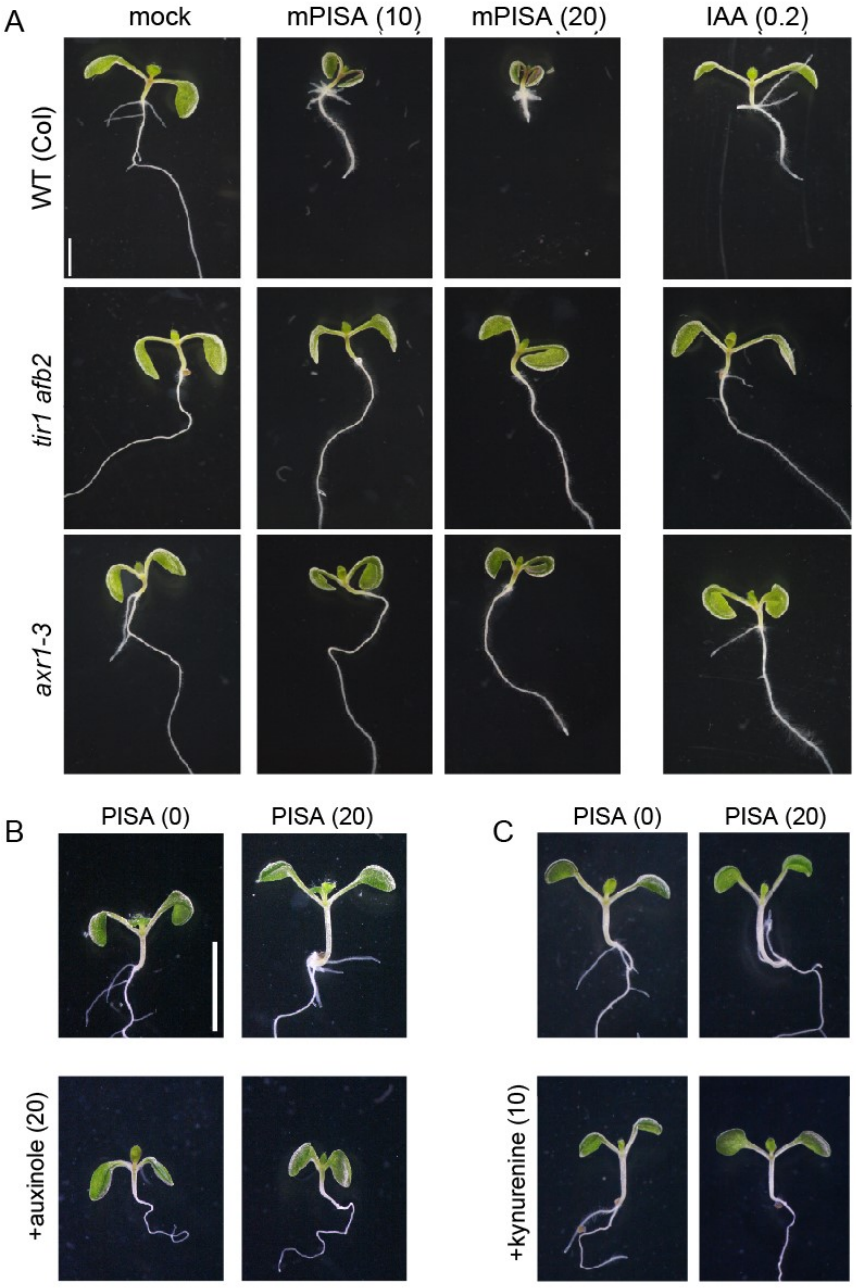

Figure S4. Effects of mPISA and PISA on the phenotype related to $SCF^{TIR1/AFB}$ pathway.

A, Phenotype of wild type, *tir1 afb2* and *axr1-3* mutant treated with mPISA. The seedling was germinated and cultured for 7 days with mPISA. The *tir1 afb2* and *axr1-3* mutants displayed severe resistant to mPISA, indicating mPISA is weak auxin. Bar represents 5 mm. (B and C) Phenotype of 7-d old seedling grown with PISA in the presence or absence of auxinole, TIR1/AFB antagonist B, and L-kynurenine, IAA biosynthesis inhibitor C, Auxinole and L-kynurenine treatment abolished PISA-induced hypocotyl elongation and adventitious root formation. Bar represents 5 mm.

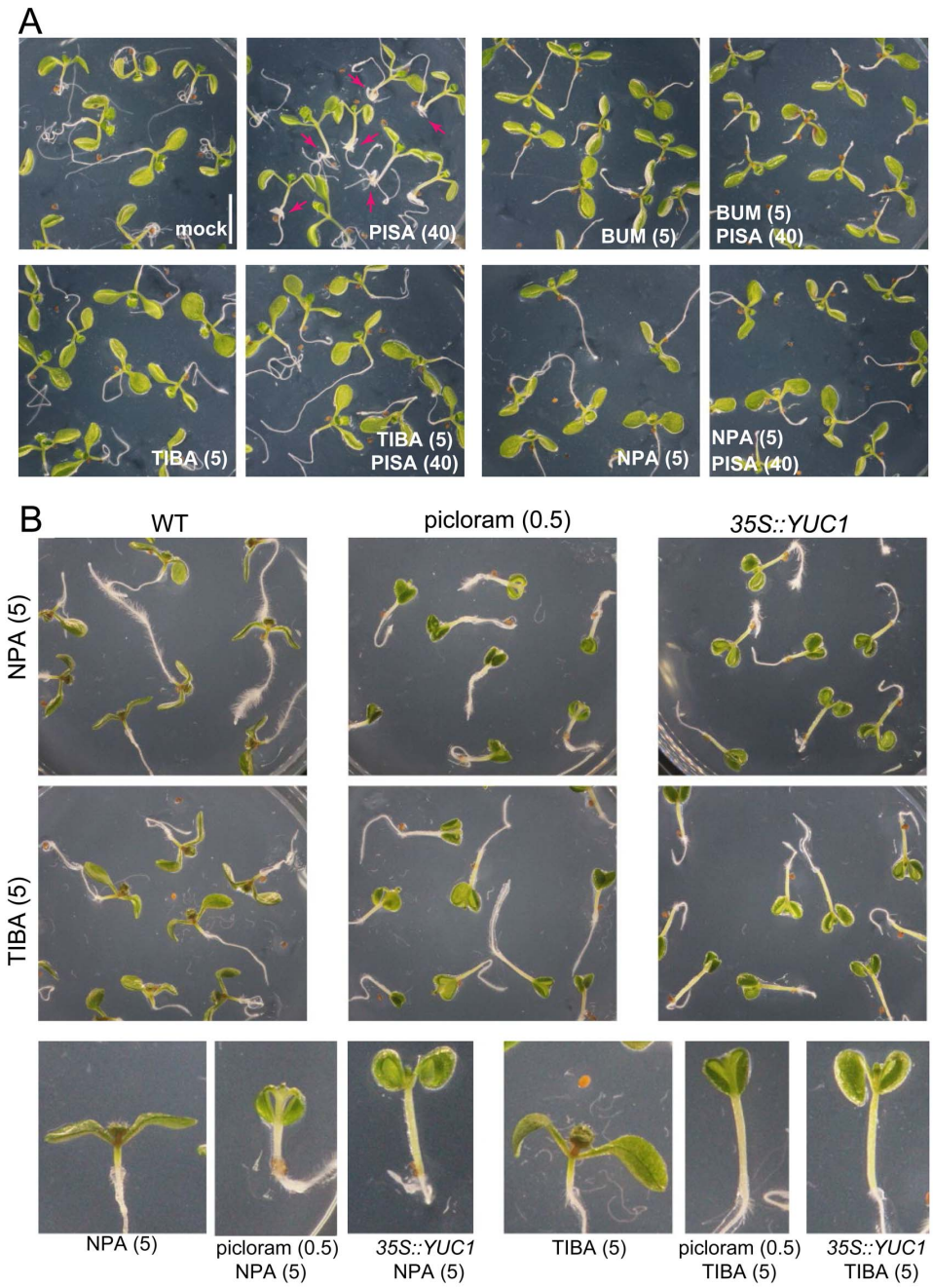

Figure S5. Auxin transport inhibitors blocked PISA-induced high-auxin phenotype, but did not inhibit the high-auxin phenotypes by picloram and YUC1 overexpression.

A, Effects of auxin transport inhibitors, BUM, NPA and TIBA on the PISA-induced hypocotyl elongation and adventitious root formation. Seedlings were germinated and cultured for 7 days with PISA and inhibitors. Arrows indicate adventitious roots. Bar represents 5 mm. B, Effects of NPA and TIBA on the high-auxin phenotype induced by picloram and YUC1 overexpression (*35S::YUC1*). The seedlings were cultured for 7 days with chemicals. Picloram and YUC1 overexpression caused typical high auxin-phenotype, hypocotyl elongation. Auxin transport inhibitors, NPA and TIBA could not restored hypocotyl elongation by picloram and YUC1 overexpression. The values in the parentheses represent the concentration of chemicals (μM).

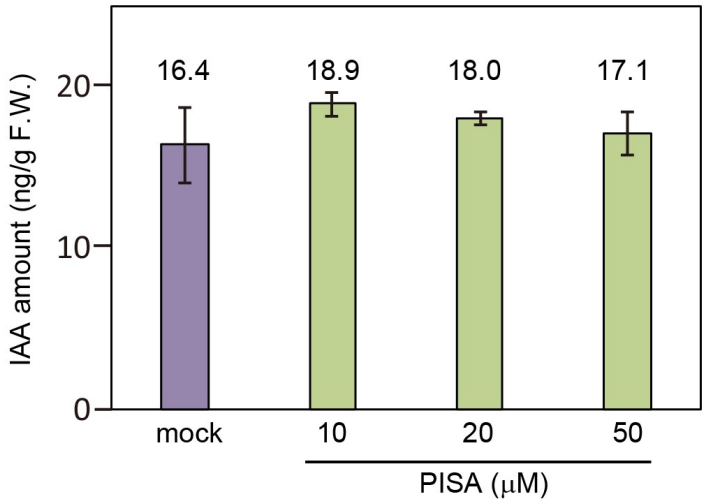

Figure S6. Effects of PISA on endogenous IAA level.

5-d-old wild-type seedlings were incubated with PISA in liquid GM medium for 16 h. The seedlings (n = 5–8) were pooled for each sample, and three samples were analyzed for each data point. Endogenous IAA levels were measured using LC-MS/MS (ng/gFW). Values are the means ± S.D.

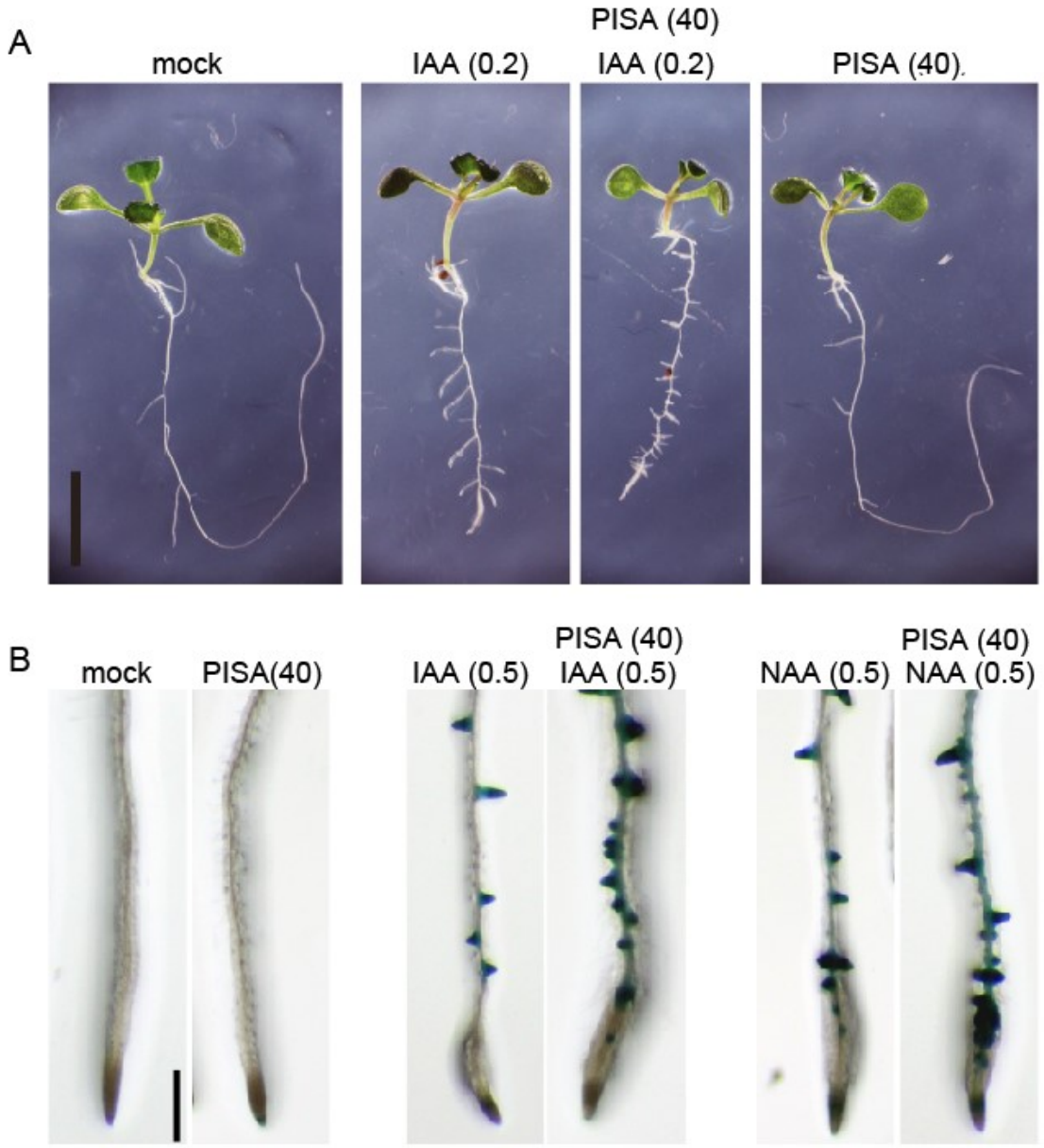

Figure S7. Phenotype of Arabidopsis seedlings co-cultured with PISA and auxins.

A, PISA promoted IAA-induced lateral root formation. PISA alone did not induce lateral root formation. 5d-old seedlings were cultured for additional 3 days with PISA in the presence of IAA. Bar represents 5 mm. B, PISA promoted auxin induced *CYCB1;1::GUS* expression (Colon-Carmona et al., 1999). 5d-old *CYCB1;1::GUS* seedlings were cultured for additional 2 days with PISA in the presence of auxins (IAA and NAA). The value in the parentheses represents the concentration of chemicals (μM).

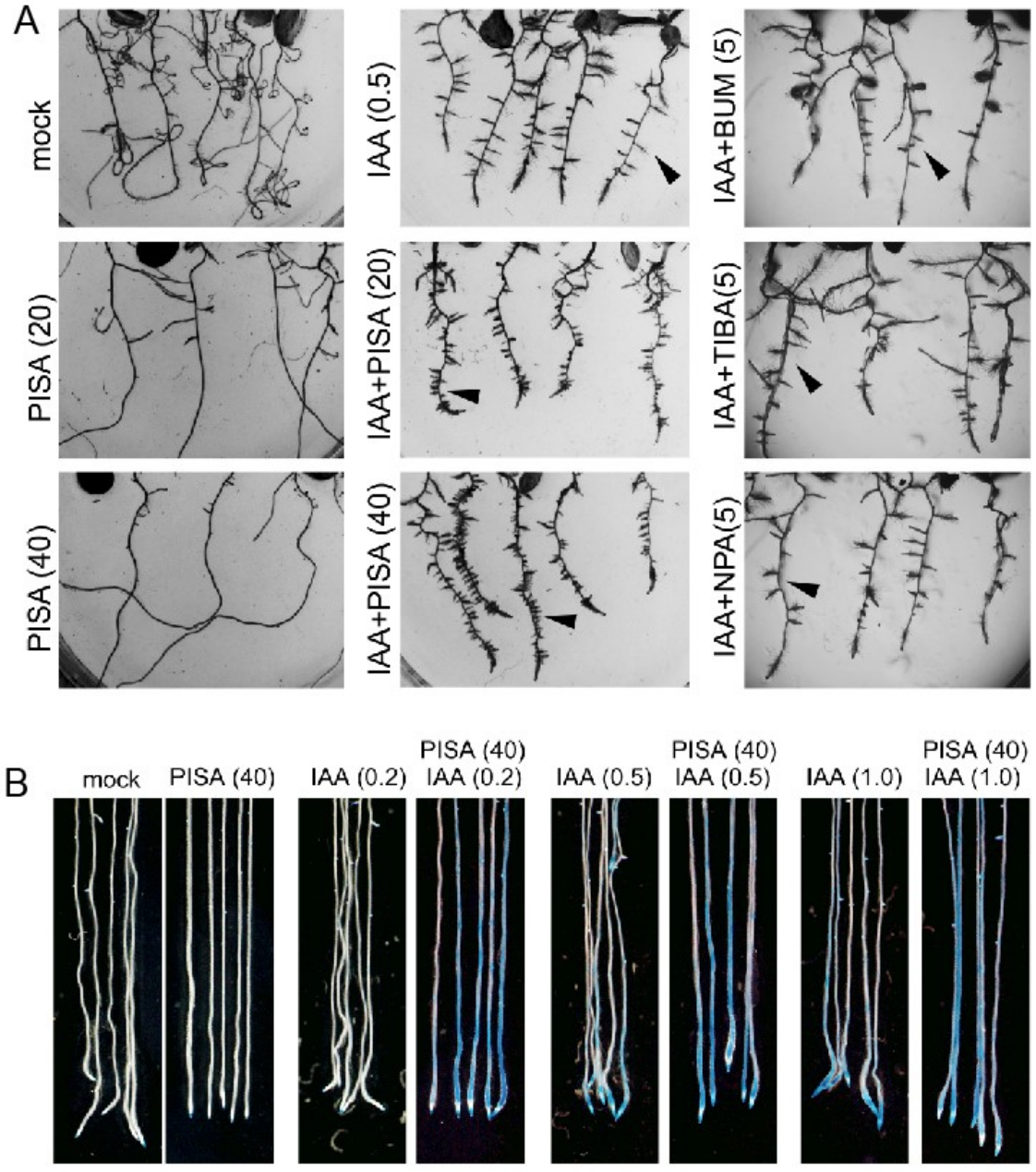

Figure S8. Effects of PISA and auxin transport inhibitors on auxin response in root.

A, Auxin transport inhibitors, BUM, TIBA and NPA did not promote IAA-induced lateral root formation. 5d-old seedlings were cultured for additional 3 days with PISA and auxin transport inhibitors, NPA, TIBA, and BUM in the presence of IAA. B, Effects of PISA on IAA-induced *DR5::GUS* expression. 5d-old *DR5::GUS* seedlings were incubated for 12 h in liquid GM medium with or without PISA. IAA was added to the GM medium and the seedlings were further incubated for additional 6 h. The values in the parentheses represent the concentration of chemicals (μM).

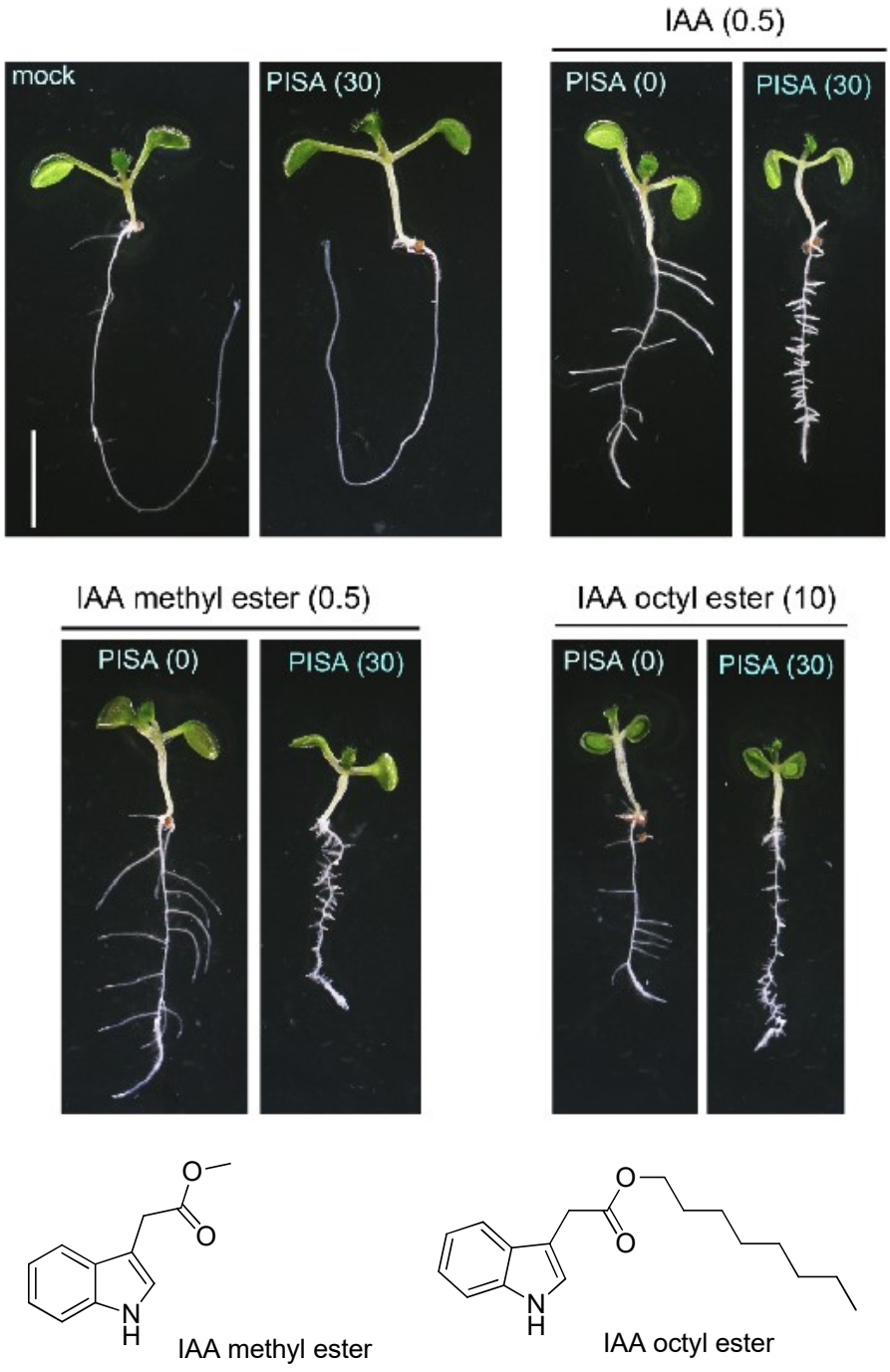

Figure S9. PISA promotes lateral root formation induced by membrane permeable IAA precursors.
5d-old seedlings were cultured for additional 3 days with PISA and the membrane permeable IAA precursors, IAA methyl ester and IAA octyl ester. In all cases, lateral root formation was increased indicating that AUX1/LAX-mediated auxin influx is not a target of PISA activity with respect to lateral root formation. The values in the parentheses represent the concentration of chemicals (μM). Bar represents 5 mm.

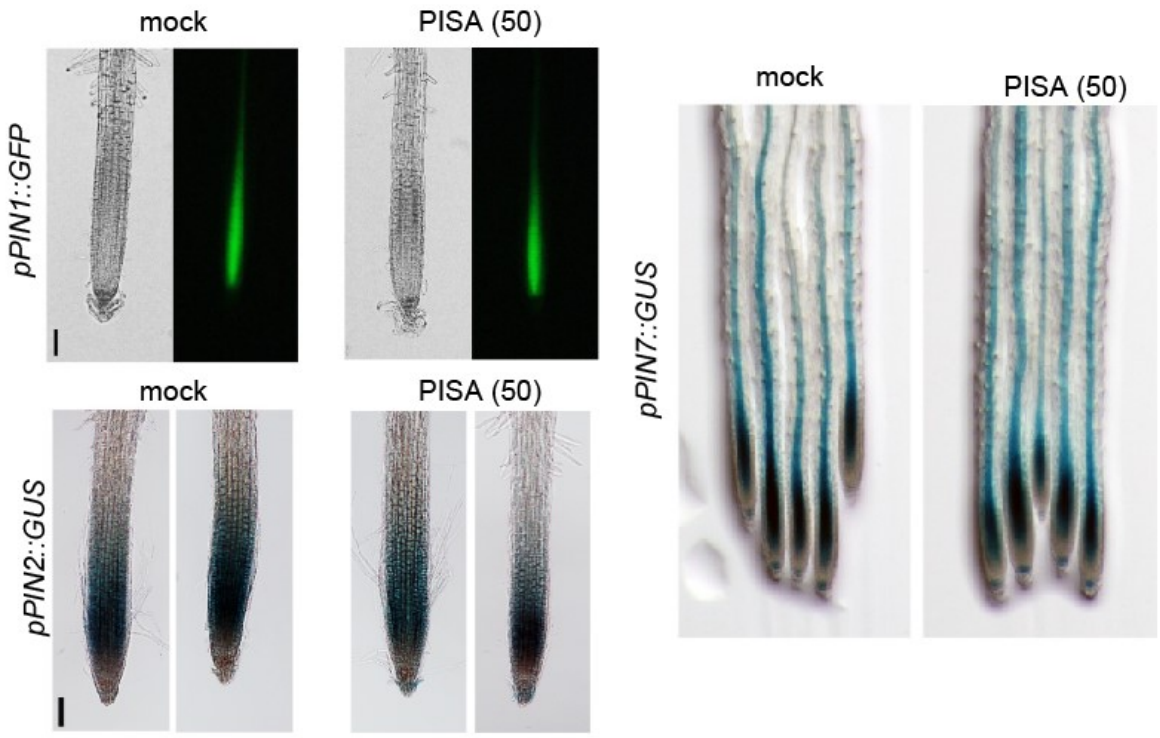

Figure S10. PISA does not affect the expression of *PIN1::GFP*, *PIN2::GUS* and *PIN7::GUS* reporter expression.

5-d old seedlings were cultured with 50 μM PISA for 18h. After the incubation, GUS lines was histochemcally stained by X-Gluc, and incubated at 37°C until sufficient staining developed. The GFP expression was recorded by fluorescent microscopy. PISA did not affect expression of reporter protein in *PIN1::GFP, PIN2::GUS,* and *PIN7GUS* lines. The values in the parentheses represent the concentration of chemicals (μM). Bar represents 100 μm.

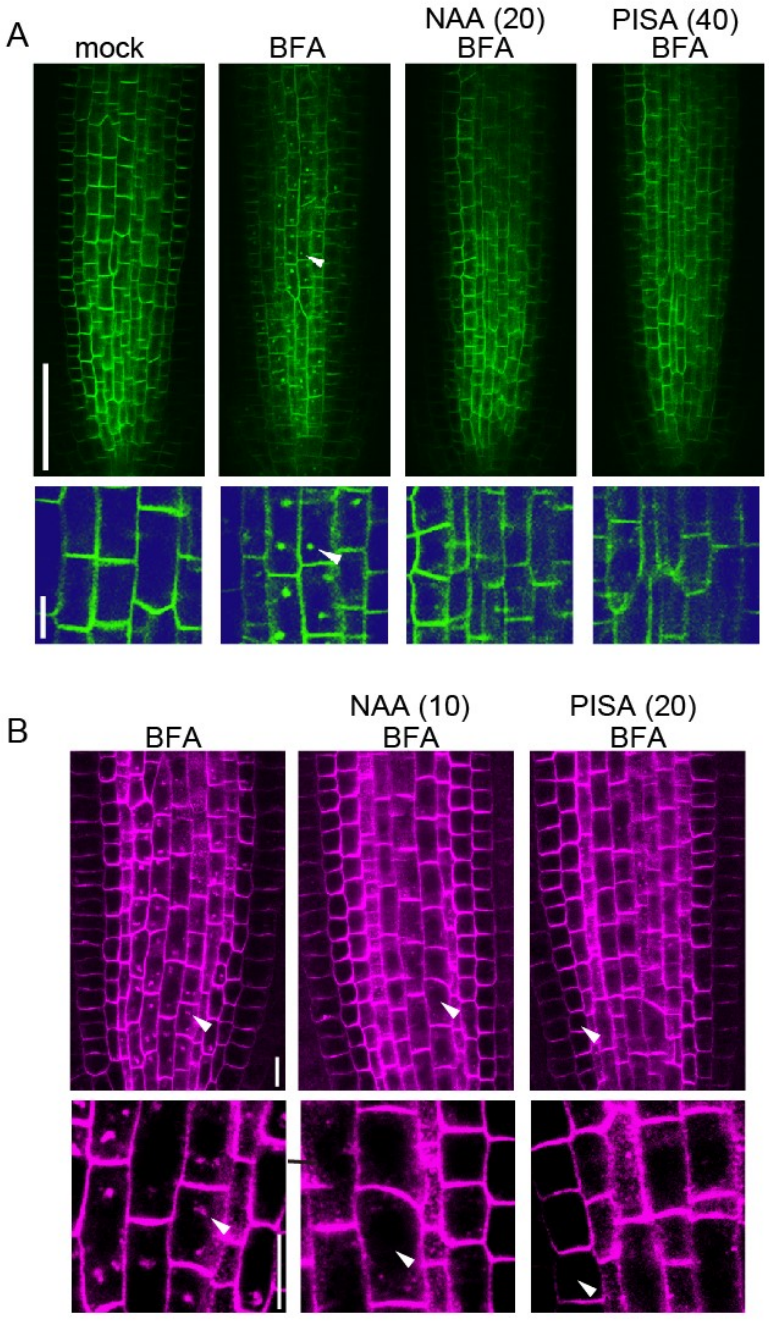

Figure S11. Effect of PISA on the BFA body formation of PIN1

A, 5d-old *proPIN1::PIN1-GFP* seedling was incubated for 30 min in liquid GM medium containing PISA and NAA, and then BFA (40 μM) was added to the medium. The seedling was incubated for additional 60 min. Bar represents 50 μm for upper panel and 5 μm for lower panel. B, 5d-old wild-type seedling was incubated for 30 min with NAA or PISA, and then the seedlings were co-treated for additional 30 min with BFA (25 μM). PIN1 protein was detected by anti-PIN1 immunolocalization. PISA and NAA inhibited the BFA-induced body formation of PIN1. Bar represents 10 μm.

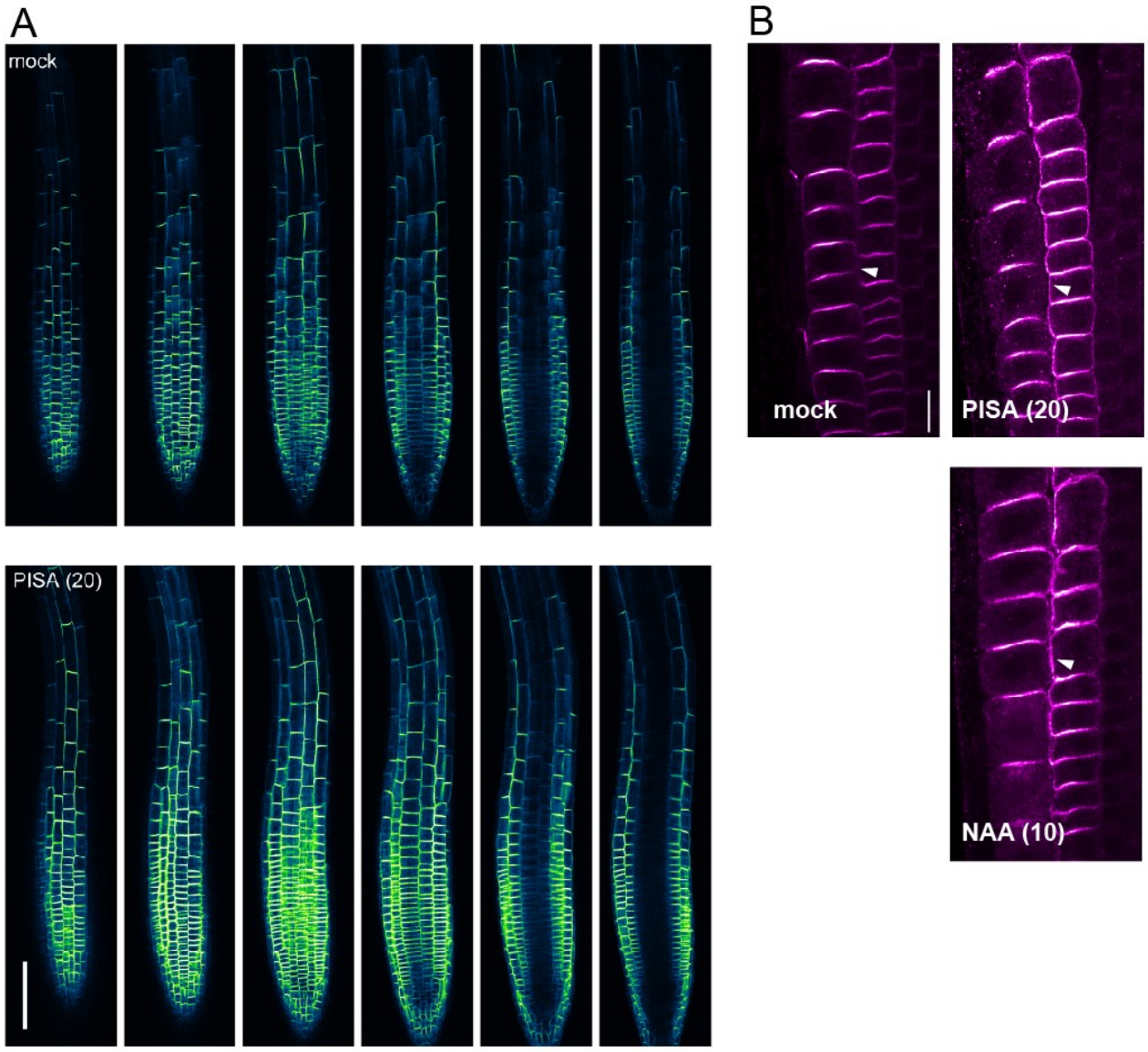

Figure S12. Effect of PISA on the internalization of PIN2-GFP.

A, 5d-old *pPIN2::PIN2-GFP* seedlings were incubated for 16h with PISA. The confocal sliced image at Z-section was obtained at each 4 μm intervals. Fluorescent signal is shown pseudo-colored. Bar represents 100 μm. B, PIN2 protein was detected by immunolocalization analysis after 4h treatment of NAA or PISA. Arrowheads indicate the accumulated PIN2 at lateral side of cell. NAA and PISA promoted the accumulation of PIN2 at the lateral side of PM. The values in the parentheses represent the concentration of chemicals (μM). Bar represent 10 μm.

.

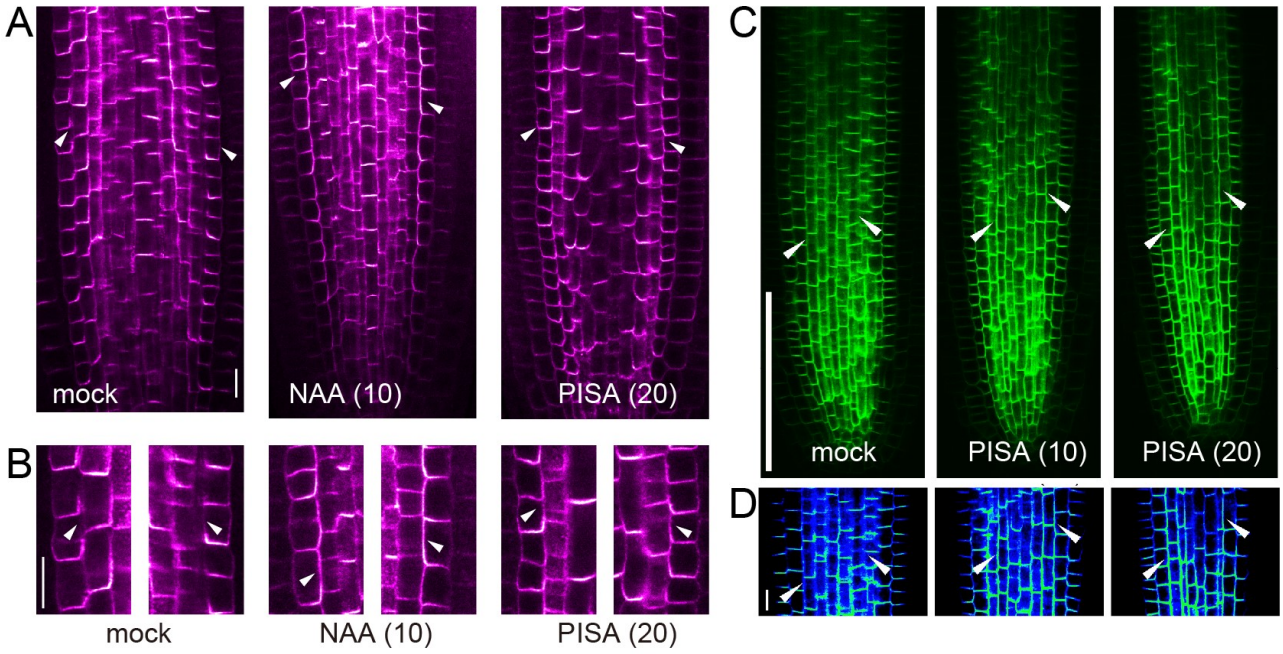

Figure S13. Effect of PISA on the internalization of PIN1.

A and B, 5d-old wild-type seedling was incubated for 4h with PISA or NAA. B, Expanded pictures for the upper pictures in A, PIN1 was analyzed by immunolcaliztion using anti-PIN1 antibody. Arrowheads indicate the lateral side of cells. PISA and NAA promoted PIN1 protein accumulation at the lateral side of endodermal cells. Bar represents 10 μm. C and D, 5d-old *proPIN1::PIN1-GFP* seedling was incubated for 11h with PISA. PISA accumulated PIN1-GFP protein at the lateral sides of cells. Arrowheads indicate the lateral accumulation of PIN1. Values in the parentheses represent the concentration of chemicals (μM). Bar represents 100 μm (panel C) and 10 μm (panel D).

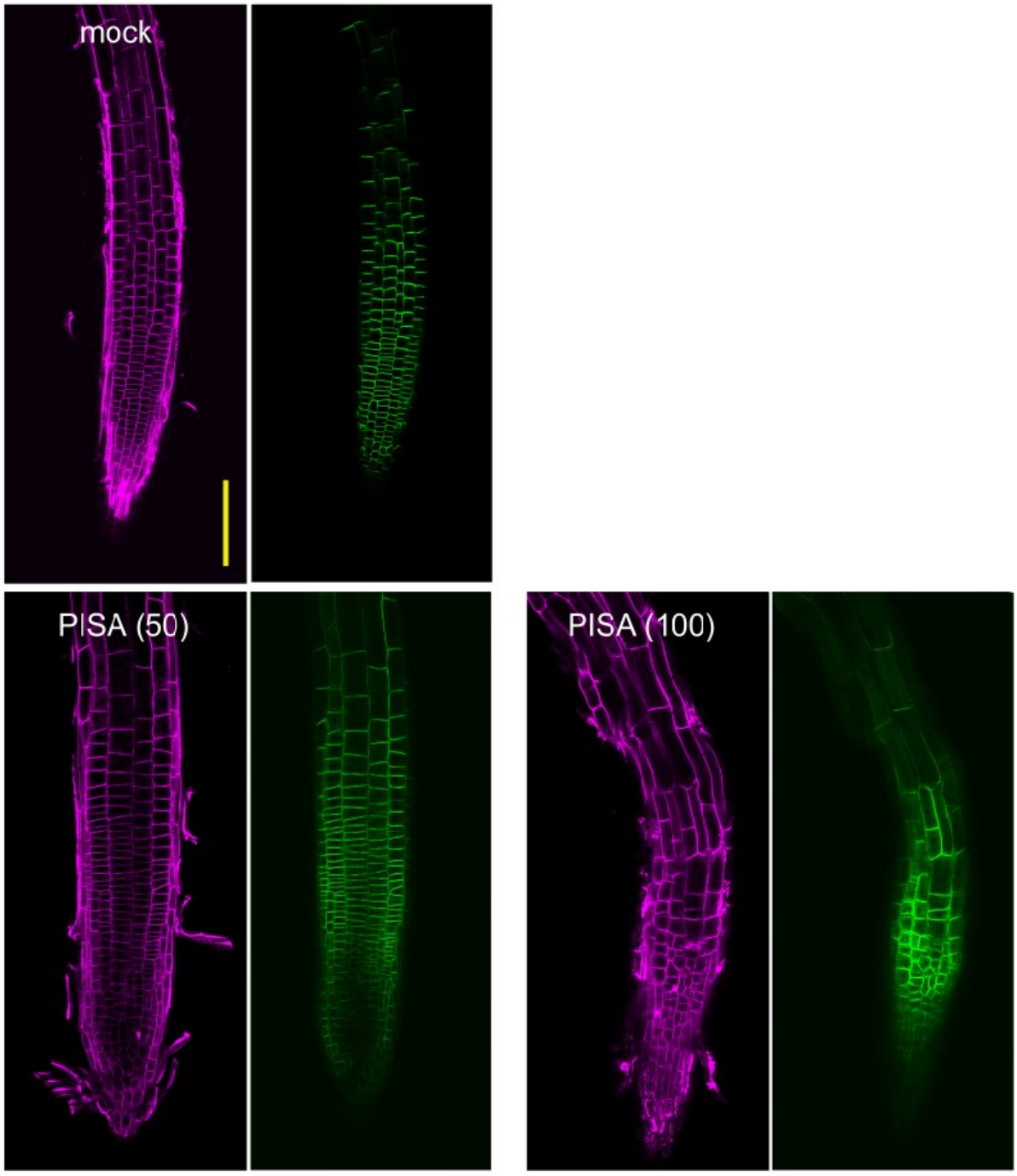

Figure S14. Effect of PISA on the internalization of PIN2 at high concentration

proPIN2::PIN2-GFP seedling was cultured for 6 days with PISA. The root was counterstained with propidium iodide (PI: magenta). The root treated with 100 μM PISA showed severe defects in root structure and PIN2-GFP localization. Values in the parentheses represent the concentration of chemicals (μM). Bar represents 100 μm.

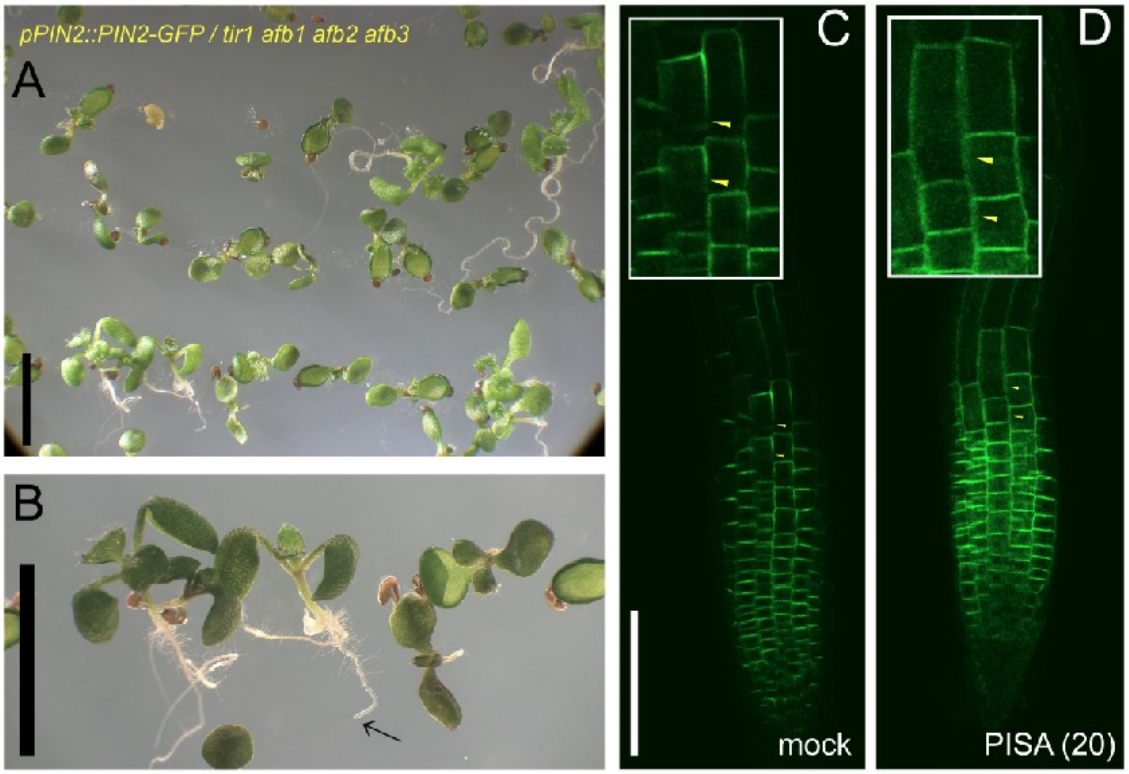

Figure S15. Effects of PISA on PIN2 membrane localization in *tir1 afb1 afb2 afb3* mutant
A and B, The *tir1 afb 1 afb 2 afb3* mutant expressing *pPIN2::PIN2-GFP* was cultured for 9 days. Bars represent 5 mm. C and D, 9-d old mutants were incubated for 12h in liquid GM medium containing PISA. The PIN2-GFP signal in root was recorded with confocal microscopy. PIN2-GFP protein accumulated at lateral side of cell following PISA treatment. The value in the parentheses represents the concentration of chemicals (μM). Bar represents 100 μm.

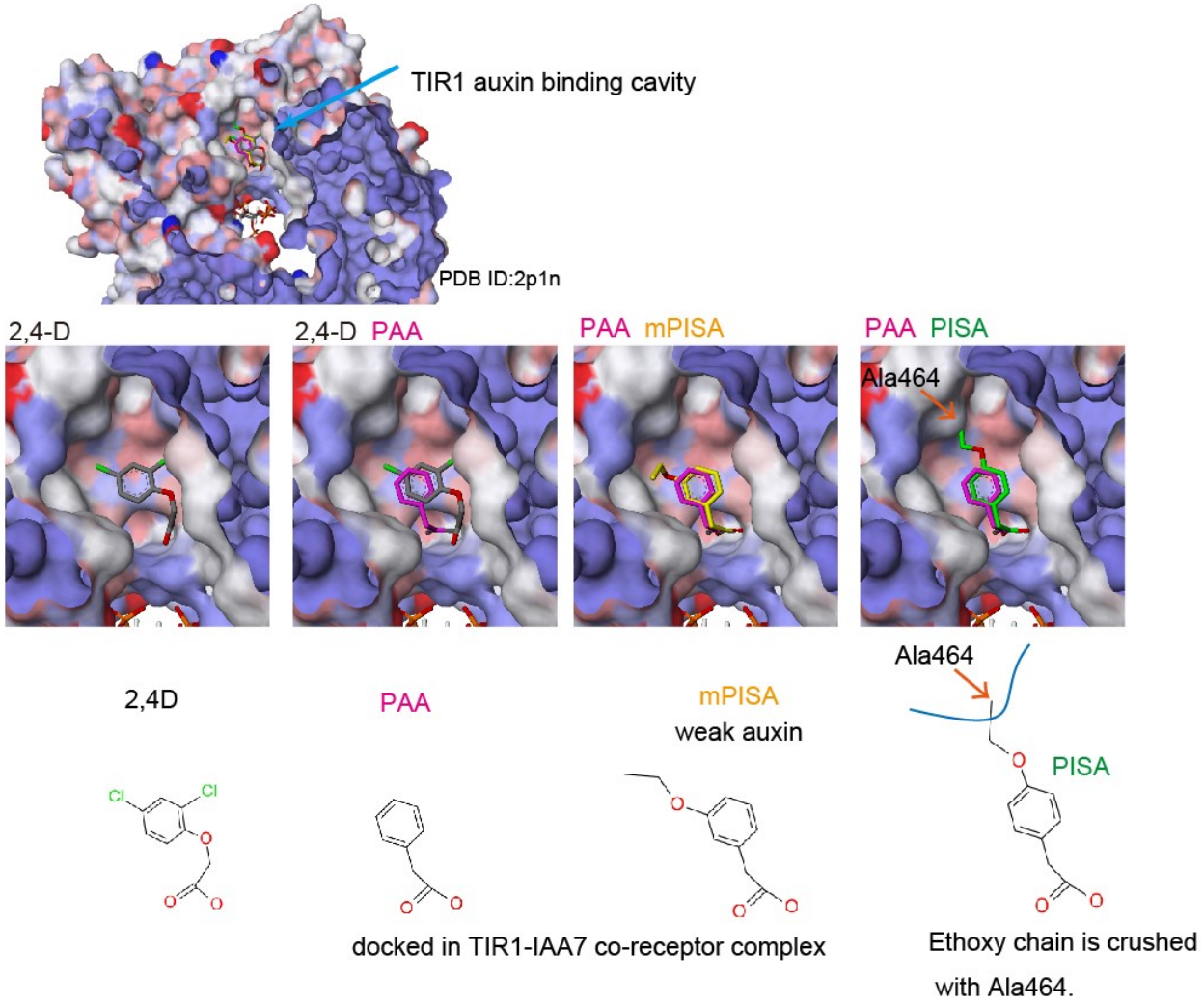

Figure S16. Molecular docking study of PAA, mPISA and PISA with TIR1.

Docking study was performed by Autodock Vina software (Trott and Olson, 2010). The binding conformation of 2,4-D and TIR1 structure was obtained from the crystal structure (PDB: 2p1n). The ligands were docked within the binding cavity of TIR1-IAA7 co-receptor complex from 2p1n.The predicted binding pose of top-scored poses of PAA and mPISA were visualized as cyan and yellow molecules, respectively. IAA7 was not shown. PISA, green colored molecule was not fitted well to binding cavity when the same coordinates as PAA and mPISA were imposed. The 4-ethoxy chain of PISA would clash with Ala464 of TIR1 auxin binding site, suggesting PISA could not stably bind TIR1 in the auxin binding cavity formed by TIR1-IAA7 complex

Supplemental Methods

Tobacco BY2 suspension cell culture.

Tobacco (Nicotiana tabacum) BY2 cells were obtained from the Riken Bioresource Center, Japan. Suspension-cultured tobacco cells (cv BY2) were maintained in a modified Murashige and Skoog medium as described previously (Winicur et al., 1998) on a rotary shaker (100 rpm) at 25°C in the dark. Auxin deprivation was carried out by washing a 7-d culture twice with the same medium lacking 2,4-D and then culturing in auxin-free medium for 24 h before auxin addition and determination of mitotic indices over time. Mitotic index of BY2 cells was determined as described previously (Winicur et al., 1998).

Pull-Down Assay with Aux/IAA Domain II Peptide and FLAG-Tagged TIR1

Pull-down assays with the biotinylated domain II peptide were performed as described previously (Kepinski, 2009; Hayashi et al., 2012). Briefly, 10 μM IAA and 50 μM PISA were added directly to the extracts of transgenic plants expressing TIR1-FLAG fusion protein containing biotinylated IAA7 domain II peptide (biotinyl-NHAKAQVVGWPPVRNYRKN-COOH) and immobilized on streptavidin agarose. After 60 min incubation at 4°C, streptavidin beads were collected and washed three times for for 5 min in extraction buffer (0.15 M NaCl, 0.5% Nonidet P40, 0.1 M Tris-HCl pH 7.5, containing 1 mM phenylmethylsulfonyl fluoride, 1μM dithiothreitol, 10 μM MG132), resuspended in SDS-PAGE sample buffer, and subjected to SDS-PAGE electrophoresis and immunoblotting with anti- FLAG antibody.

Rapid Hypocotyl elongation assays:

Hypocotyl elongation assay was performed essentially same procedure as previously described (Takahashi et al., 2012). Briefly, the hypocotyl sections (ca. 4 mm) excised from 3-d-old etiolated seedlings were incubated on growth medium (10 mM KCl, 1 mM MES-KOH [pH 6.0], and 0.8% agar) for 0.5 to 2.0 h in darkness to deplete endogenous auxin. The preincubated hypocotyl sections were

then cultured in the growth medium containing IAA or PISA at the indicated concentrations. The hypocotyl sections were image-captured with a digital camera immediately and 30 min after being transferred onto the test medium. The hypocotyl elongation for 30 min was measured with image J software (n= 15 hypocotyl sections). Experiments were repeated at least three times.

Measurements of endogenous IAA

LC-ESI-MS/MS analysis of IAA was performed using an Agilent 6420 Triple Quad system (Agilent) as previously described (Mashiguchi et al., 2011)

References in Supplemental Methods

Colon-Carmona A, You R, Haimovitch-Gal T, Doerner P (1999) Technical advance: spatio-temporal analysis of mitotic activity with a labile cyclin-GUS fusion protein. Plant J **20:** 503-508

Hayashi K, Neve J, Hirose M, Kuboki A, Shimada Y, Kepinski S, Nozaki H (2012) Rational design of an auxin antagonist of the SCF(TIR1) auxin receptor complex. ACS Chem Biol **7:** 590-598

Kepinski S (2009) Pull-down assays for plant hormone research. Methods Mol Biol **495:** 61-80

Mashiguchi K, Tanaka K, Sakai T, Sugawara S, Kawaide H, Natsume M, Hanada A, Yaeno T, Shirasu K, Yao H, McSteen P, Zhao Y, Hayashi K, Kamiya Y, Kasahara H (2011) The main auxin biosynthesis pathway in Arabidopsis. Proc Natl Acad Sci U S A **108:** 18512-18517

Nishimura K, Fukagawa T, Takisawa H, Kakimoto T, Kanemaki M (2009) An auxin-based degron system for the rapid depletion of proteins in nonplant cells. Nat Methods **6:** 917-922

Oono Y, Chen QG, Overvoorde PJ, Kohler C, Theologis A (1998) age Mutants of Arabidopsis exhibit altered auxin-regulated gene expression. Plant Cell **10:** 1649-1662

Takahashi K, Hayashi K, Kinoshita T (2012) Auxin activates the plasma membrane H+-ATPase by phosphorylation during hypocotyl elongation in Arabidopsis. Plant Physiol **159:** 632-641

Trott O, Olson AJ (2010) AutoDock Vina: improving the speed and accuracy of docking with a new scoring function, efficient optimization, and multithreading. J Comput Chem **31:** 455-461

Winicur ZM, Zhang GF, Staehelin LA (1998) Auxin deprivation induces synchronous Golgi differentiation in suspension-cultured tobacco BY-2 cells. Plant Physiol **117:** 501-513